이자율 기간구조를 이용한 기준금리 공시 효과 분석

송 준 혁*

< 초 록 >

.

* 한국외대 경제학과 교수, jhsong@hufs.ac.kr

Ⅰ. 서 론

우리 경제는 고령화의 진전과 계약성 저축이 증가함에 따라 안정적인 장기투자 수단에 대한 수요가 높아지는 가운데 금융기관들도 자산 운용 대상 및 위험관리 수단으로서의 채권의 수요가 증가하고 있다. 이러한 상황을 감안할 때 채권시장에 대한 전반적인 이해와 채권가격을 결정짓는 이자율 기간구조를 살펴보는 것은 상당히 중요한 과제이다. 특히 2008년 글로벌 금융위기 이후 과도하게 팽창된 유동성이 인플레이션을 견인함에 따라 이자율이 상승함에 따라 채권 투자에 대한 수요가 증대하는 가운데 향후 이자율 움직임에 대한 정책 당국과 민간 투자자들의 관심이 고조되고 있다.

이자율 기간구조(term structure of interest rates)는 채권의 수익률(만기수익률, 현물이자율, 선도이자율)과 만기 사이의 관계를 의미한다. 이자율 기간구조는 어떤 특정 시점에서 향후 시장이 예상하고 있는 이자율 변화의 크기와 방향에 대한 정보를 담고 있으며 이러한 정보에는 미래 경제상황에 대한 경제주체들의 다양한 기대가 반영되어 있다. 또한 모든 금융자산의 가격결정에는 이자율이 직간접적으로 영향을 미치고 있다는 점을 감안할 때 정확하고 신뢰성 높은 이자율 기간구조는 금융상품 및 금융시장의 발전과 긴밀하게 연관되어 있다. 즉 금융시장 참가자들은 이자율 기간구조를 채권 포트폴리오의 운영이나 이자율 및 신용 관련 파생상품의 가치 평가, 이자율 위험의 관리 또는 헤징의 수단으로서 사용하고 있다. 또한 통화정책 당국자의 입장에서도 이자율 기간구조는 시장에서 예상하고 있는 미래의 이자율 및 인플레이션에 대한 예측에 대한 정보를 담고 있으므로 향후 통화정책의 방향을 설정하는 데 유용한 정보 변수로서의 기능을 수행할 수 있다.

Vasicek(1977) 이후 파생금융상품의 가치 평가에 대한 관심이 증대되는 과정에서 이자율 기간구조에 대한 많은 연구들이 진행되어 왔다. 특히 Cox, Ingersoll and Ross(1985)가 투자자의 위험 기피 및 시간 선호 등을 고려한 일반균형(general equilibrium)하에서의 단기이자율의 확률적 움직임을 이론적으로 도출함에 따라 이자율 기간구조에 대한 이론적 연구는 비약적으로 발전하게 되었다. 이후 Duffee and Kan(1996), Dai and Singleton(2000), Duarte(2000), Kim and Orphanides(2006) 등에서는 채권 수익률에 영향을 미치는 비관측 상태변수를 상정하고 이를 이용하여 이자율 기간구조를 추정하는 모형을 소개하였다. 최근

들어서는 이러한 상태변수가 거시변수와의 연관성이 강조되는 연구가 진행되고 있는데 대표적인 연구로는 Bekaert, Cho and Moreno(2005), Ang, Piazzesi and Wei(2006), Rudebusch and Wu(2008), Doh(2009) 등을 들 수 있다.

본 연구에서는 우리나라 국고채와 신용채(회사채 AA-등급)를 이용하여 무차익거래 조건하에서 3요인 선형 가우시안 이자율 기간구조모형을 추정하고 이를 이용하여 최근의 정책금리 변경의 효과성에 대해 진단해 보고자 한다. 2015년 이후 최근까지 한국은행의 기준금리는 19차례나 변경됨에 따라 2015년 3월의 1.75%에서 2023년 1월에는 3.5%로 상승하였다. 기준금리의 총량적인 변화를 8년 정도의 기간에 걸쳐 1.75%p 상승하였으나 이를 기간별로 분해해 보면 2015년 3월에서 2020년 5월까지는 추세적인 금리 하락 기조가 만연한 반면 이후에는 금리 상승 기조로 반전하여 최근의 금리 수준에 이르렀다.[1)]

이자율 기간구조에서의 장기이자율은 미래 기대 단기이자율과 인플레이션 혹은 유동성 리스크에 대한 보상을 나타내는 기간프리미엄(term premium)으로 분해할 수 있다. $y_t(n)$과 $y_t(1)$을 각각 t시점에서의 무이표채(zero-coupon bond)에 대한 n기 만기 이자율(장기이자율) 및 1기 만기 이자율(단기이자율)이라고 하면 장기이자율은 다음과 같이 기대 단기이자율의 평균과 기간프리미엄(TP)으로 분해할 수 있다.

$$y_t(n) = \frac{1}{n}\sum_{j=0}^{n-1} E_t y_{t+j}(1) + TP_t(n)$$

이자율 기간구조의 이론 중 하나인 기대가설하에서는 기간 프리미엄은 상수, 즉 $TP_t(n) = TP(n)$이므로 장기이자율의 변화는 미래에 예상되는 단기이자율의 평균의 변화에서 비롯되는 것으로 인식되었다. 단기이자율은 중앙은행의 정책금리에 가장 영향을 많이 받기 때문에 기대가설하에서는 장기이자율은 결국 중앙은행의 미래 정책금리에 대한 기대를 반영하는 것을 의미하게 된다. 중앙은행의 정책금리는 경기 및 물가에 영향을 받아 결정되므로 결국 장단기 이자율 스프레드가 거시경제에 대한 기대 정보가 반영되게 된다.

그러나 Fama and Bliss(1987)의 연구 결과에 따르면 채권의 기간프리미엄은 시변(time-varying)하는 것으로 알려졌고 이에 따라 전통적인 기대가설은 더 이

1) 2020년 5월 28일에는 기준금리가 0.5%로 최저치를 보인 이후 2021년 8월 26일에 기준금리가 0.75%로 상승한 이후 2023년 1월 13일에는 3.5%를 보이고 있어 금리 하락 후 상승 반전이 가빠르게 진행되고 있음을 알 수 있다.

상 성립하는 않는 것으로 밝혀졌다. Rudebusche et al.(2007), Ludvigson and Ng에서는 기간프리미엄이 경기 역행성을 가진다고 주장하고 있다. 한편 Gurkaynak and Wright(2012)에서는 기간프리미엄이 인플레이션과 양(+)의 상관관계를 가진다고 주장하는 등 최근에는 미래의 기대 단기이자율보다는 기간프리미엄의 경기 예측력이 높다는 분석 결과가 다수를 이루고 있다.

본고에서는 먼저 장단기 이자율 스프레드를 기대 스프레드와 기간프리미엄으로 분해하여 최근의 국고채 및 신용채 시장에서의 장단기 금리 스프레드가 어느 요인에 의해 더 큰 영향을 받았는지를 살펴보고자 한다. 이와 더불어 정책금리 변경 시점을 전후하여 정책금리의 변동이 주로 미래의 기대 단기이자율에 영향을 미치는지 아니면 기간프리미엄에 영향을 미치는지도 같이 살펴보고자 한다. 이러한 이자율 분해를 통해 중앙은행의 정책금리 변경이 실물 및 금융에 미치는 경로에서 어떤 채널이 더 유효하고 의미있는지를 실증적으로 제시하는 것은 금리 정책의 유용성을 제고하는데 기여할 수 있을 것이다.

이자율 기간구조와 관련된 국내의 연구로는 이병근 · 현정순(2002)은 Heath-Jarrow-Morton 모형을 이용하여 통화안정증권을 기준으로 수익률 곡선을 추정하였다. 한편 김명직 · 장국현(2000)에서는 다요인 CIR모형을 이용하여 통화안정증권을 통해 수익률곡선을 추정한 바 있으며 김명직 · 신성환(2001)에서는 상태-공간모형을 이용하여 국민주택채권을 기준으로 수익률곡선을 추정한 바 있다. 이상의 연구는 수익률곡선의 추정에 일차적인 관심을 가지고 있어서 구체적으로 추정된 수익률곡선이 경제현상을 어떻게 설명할 수 있는 지에 대한 논의는 결여되어 있었다. 엄영호 · 이준희 · 지현준(2007)은 2요인 확장 가우시안 모형을 통해 수익률 곡선을 추정하였으며 정책금리의 변경이 단기이자율 및 단기이자율의 정상상태 평균에 미치는 영향에 대해 분석하였는데, 분석 결과 우리나라의 단기이자율은 콜금리 인하의 경우에서의 반응 정도가 인상의 경우보다는 더 크게 나타난다고 주장하였다. 송준혁(2009)에서는 3요인 무차익거래 모형을 상정하여 이자율 기간구조를 추정하고 단기이자율 형성에 있어서의 정책금리의 효과보다는 신호 기능(signalling) 측면에서 정책금리의 유효성을 살펴본 바 있다. 윤재호(2020)에서는 이자율 스프레드가 산업생산 증가율, 소비자물가 상승률, 생산갭 등 주요 거시경제변수들에 대한 유의한 예측력을 가지고 있었다. 그러나 인플레이션 타겟팅 강화로 인해 이자율 스프레드의 경기 예측력이 전반적으로 저하되고 있으나 기간프리미엄의 경기 예측력은 여전히 유의하다고 분석한 바 있다.

아래에서의 논문 구성은 다음과 같다. 먼저 2장에서는 3요인 무차익거래 조건하에서의 이자율 기간구조 모형을 설정하였다. 본고에서는 국고채와 같이 무위험 채권만을 대상으로 한 모형과는 차별화하여 국고채와 신용채를 모두 포함한 이자율 기간구조 모형을 상정하고자 한다. 3장에서는 사용된 자료와 추정 결과를 제시하였다. 그리고 4장에서는 이자율 기간구조에서 도출된 단기이자율 및 현물수익률을 이용하여 최근의 통화정책의 효과성에 대한 분석을 시도하였으며 결론은 5장에 제시하였다.

II. 이자율 기간구조 모형

이자율기간구조는 모형의 형태와 변수의 선정이라는 두 가지 방향에 초점을 모을 수 있다. 우선 모형의 형태와 관련해서는 재무이론에서 다루는 초단기 이자율(instantaneous short rate)을 확률과정(stochastic process)으로 가정하고 분석하고자 한다. 이러한 확률과정에서 가장 많이 사용되는 모형은 Ornstein-Uhlenbeck 과정이라고 부르는 Gaussian process인데 본고에서도 이 과정을 기본으로 모형을 설정한다. 변수의 선정과 관련해서는 거시변수를 이용하여 모형화를 할 수도 있으나 본고에서 다루는 내용이 할인율 갭인 점을 감안하여 순수하게 금리 자료만을 사용하고 금리의 변동을 야기하는 은닉인자(latent factor)로서의 상태변수를 이용하는 요인모형을 구성하였다.

상태변수와 관련해서 모형 설정 이전에 결정해야 할 것은 상태변수의 개수인데 많은 연구에서는 3요인이 이자율기간구조의 대략 90%를 설명하고 있는 것으로 알려져 있고 요인이 증가할수록 모형 설명력은 증가하나 모형 예측력은 감소하는 특성을 가지고 있으므로 본고에서도 3요인을 상태변수의 한 확률적 이자율 모형인 선형 이자율기간구조 모형(3-factor affine term-structure model)을 설정하였다.

동 모형의 핵심은 상태변수의 동학(dynamics)과 위험의 시장가격을 어떻게 설정하는 것이다. 국채 수익률과 회사채 수익률(AA- 등급)의 모형화를 위해 초단기 무위험이자율(risk-free instantaneous short rate), $r(t)$와 AA-에 해당하는 초단기 위험이자율(risky instantaneous short rate) $R(t)$를 상태변수의 선형결합으로 가정하였다. 먼저 r_t는 아래의 식과 같이 2개의 상태변수 X_1, X_2와 상수항

의 합으로 가정한다.

$$r_t = a_0 + a_1 X_{1t} + a_2 X_{2t}$$

또한 R_t는 상수항, 초단기 무위험 이자율 및 1개의 상태변수 X_3의 합으로 가정한다. 여기서 제시된 세 번째 요인인 X_3은 신용위험을 결정하는 상태변수의 기능을 담당한다.

$$R_t = b_0 + b_1 r_t + b_2 X_{3t}$$

상태변수 $X_t = [X_{1t}, X_{2t}, X_{3t}]$은 아래와 같은 가우시안 동학(Gaussian dynamics)을 갖는다고 가정하였다.

$$dX_t = -\kappa X_t dt + d W_t$$

여기에서 X_t는 3×1 벡터(vector)이며, κ는 3×3 하삼각행렬(lower triangular matrix), $W_t = [\, W_{1t}, W_{2t}, W_{3t} \,]^T$는 3×1 벡터 브라우니언 모션(Brownian motion)을 의미한다. 초단기이자율은 이론적인 개념으로 찰나의 순간에 만기가 도래하는 채권에 적용되는 이자율로 현실에서는 관찰되지 않는 이자율이다. 따라서 초단기이자율은 이론적 정합성을 위해 도입된 가상적인 이자율인데 이것이 존재한다는 가정하에서 확률적 할인요인(SDF, Stochastic Discount Factor) 또는 가격핵(pricing kernel)이 다음과 같은 확률과정을 가지는 것으로 가정한다.

$$\frac{dM_t}{M_t} = -r_t dt - \lambda_t{}' d W_t$$

여기서 위험의 시장가격(market price of risk)을 결정하는 λ_t는 상태변수에 대한 선형결합으로 다음과 같이 표현할 수 있다.

$$\lambda_t = \lambda_0 + \lambda_1 X_t$$

여기서 $\lambda(t)$와 λ_0는 3×1 벡터이며, λ_1은 3×3 행렬로서 비 대각원소들(off-diagonal terms)이 모두 0인 대각행렬(diagonal matrix)이다. 이 식이 의미하는 바는 위험의 시장가격이 매 시점 t의 상태변수 X_t의 함수로 표현된다는 것으로 시변 위험프리미엄(time-varying risk premium)의 포착을 가능하게 하며, 또한 본 모형의 상태변수 X_t가 확률적으로 움직이므로 위험프리미엄이 시간이 흐르면서 그 부호(sign)를 바꿔 취할 수도 있음을 의미한다.

만기가 T인 할인채의 t시점에서의 가격은 지금까지 가정한 선형모형의 무차익

거래조건(no arbitrage condition)에 의해 아래의 식과 같이 지수선형(exponential affine)형태의 방정식을 갖게 된다는 것이 알려져 있다.[2)]

$$P(X_t,n) = \exp(-c(n) - d(n)'X_t)$$

여기서 $n = T-t$로 만기까지 남은 기간을 의미한다. $c(n)$, $d(n)$는 아래와 같은 연립상미분방정식(system of ordinary differential equations)의 해(solution)로 표현된다.

$$\frac{\partial c(n)}{\partial t} = \rho_0 - c(n)'\lambda_0 - \frac{d(n)'d(n)}{2}$$

$$\frac{\partial d(n)}{\partial t} = \rho_1 - \kappa' d(n) - \lambda_1 d(n)$$

여기서 ρ_0는 국고채일 경우에는 a_0이고 신용채일 경우에는 $b_0 + a_0 b_1$이 되고, ρ_1은 국고채일 경우에는 $[a_1, a_2]'$이고 신용채일 경우에는 $[a_1 b_1, a_2 b_1, b_2]'$이 된다. 위 식의 채권 가격식과 상태변수의 지수 선형성, 그리고 가우시안 상태변수, X_t의 특징을 이용하면 실제 채권 자료를 통해 3요인 선형이자율 기간구조 모형의 모수들을 MLE를 통해 추정할 수 있다.

이자율에서의 기간프리미엄은 다음의 두 가지 방식으로 도출된다. 먼저 n기 만기에 해당하는 무차익거래 조건하의 기간프리미엄은 다음과 같다.

$$TP_t(n) = y_t(n) - \frac{1}{n}\sum_{j=0}^{n-1} E_t y_{t+j}(1)$$

한편 선도이자율을 고려할 경우 기간프리미엄은 다음과 같이 정의될 수 있다.

$$TP_t^{fwd}(n) = f_t(n) - E_t y_{t+n}(1)$$

이론적으로는 $TP_t(n) = TP_t^{fwd}(n)$가 성립되어야 하나 실제 자료를 이용한 추정에서는 이들 관계가 성립되지 않는 경우가 자주 목격된다. 본고에서는 두 가지 형태로 정의된 기간프리미엄을 모두 제시하고자 한다.

Ⅲ. 분석 자료 및 추정

1. 분석 자료

2) 이에 대한 자세한 설명은 Duffie and Kan(1996), Dai and Singleton(2000)을 참고하기 바란다.

이자율기간구조 모형 추정을 위해서 표본기간 2015년 1월부터 2022년 8월까지의 국고채와 AA+ 등급 무보증 회사채의 주별 자료를 이용하였다.[3] 나이스 P&I에서 제공받은 국고채와 AA+ 등급 회사채는 각각 6개의 만기(1, 2, 2.5, 3, 4, 5년물)의 매주 수요일 종가 자료를 이용하여 총 375개의 관측치를 사용하였다.

[그림 1]을 보면 2015년 이후 지속적으로 하락해 왔던 채권금리가 2021년 후반에 들어서면서 모든 만기에서 상승세로 반전되고 있음을 알 수 있다. <표 1~4>는 국고채와 AA+, AA0, AA− 등급 회사채의 기초통계량을 보여주고 있다. Jacque−Bera 정규분포 검정 결과 모든 수익률에서 정규성이 기각되고 있는 것으로 나타났다. 채권 수익률의 왜도(skewness)는 대부분 정규분포에서 벗어나 오른쪽으로 쏠린 우측 편포(skewed to the right) 특성을 보이고 있다. 채권 수익률의 첨도(kurtosis)의 경우 국고채 및 신용채의 모든 만기에서 양(+)의 값을 가지고 있어 정규분포보다 중심이 높은 뾰족한 모습을 가지는 것으로 나타났다.

3) 나이스 P&I로부터는 신용채로서 AA+, AA0, AA- 등급의 회사채 자료를 제공받았으나 분석에서는 AA-등급의 회사채를 이용하였다. 해당 자료는 일별로 입수하였으나 일별 자료를 이용할 경우 시계열의 자기상관이 높아 모수 추정이 적절히 되지 않아 주별 자료로 변환하여 사용하였다.

[그림 1] 국고채 및 신용채 이자율 시계열 구조

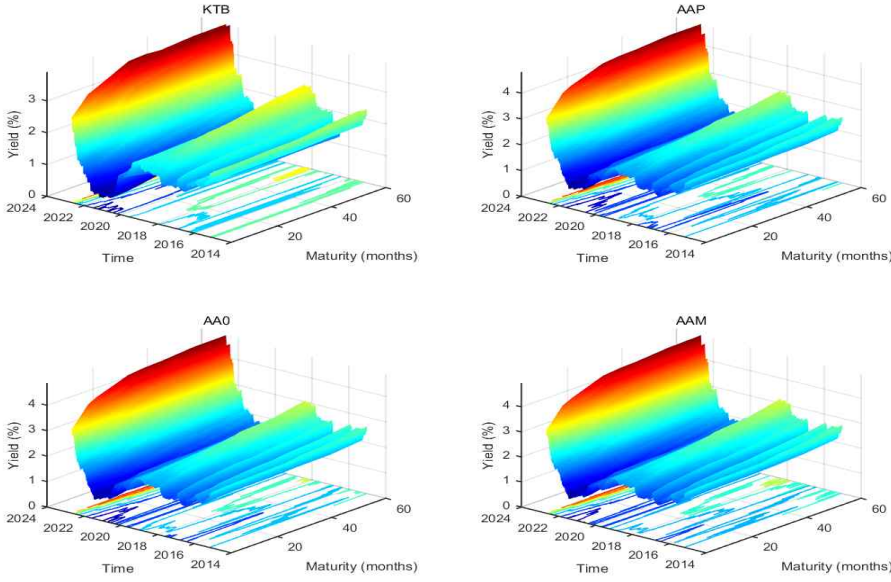

자료: NICE P&I

<표 1> 국고채 수익률 기초 통계량[1)]

(단위: %)

만기	평균	표준편차	자기상관	왜도	첨도	Jarque-Bera Test(p-value)
Y12	1.452	0.492	1.003	0.338	4.417	0.001
	(0.030)	(0.027)	(0.002)	(0.197)	(0.400)	
Y24	1.626	0.534	1.002	0.954	5.151	0.001
	(0.032)	(0.034)	(0.003)	(0.161)	(0.492)	
Y30	1.661	0.537	1.002	0.991	5.052	0.001
	(0.032)	(0.034)	(0.003)	(0.154)	(0.497)	
Y36	1.692	0.542	1.002	1.035	4.877	0.001
	(0.033)	(0.034)	(0.003)	(0.135)	(0.457)	
Y48	1.818	0.540	1.001	1.063	4.696	0.001
	(0.033)	(0.033)	(0.003)	(0.130)	(0.451)	
Y60	1.882	0.533	1.001	1.063	4.525	0.001
	(0.032)	(0.032)	(0.003)	(0.128)	(0.442)	

주: 1) ( )안은 표준오차를, Y뒤의 숫자는 개월 수를 각각 의미한다.

<표 2> AA+ 등급 회사채 수익률 기초 통계량[1)]

(단위: %)

만기	평균	표준편차	자기상관	왜도	첨도	Jarque-Bera Test(p-value)
Y12	1.767	0.530	1.005	1.620	8.275	0.001
	(0.032)	(0.045)	(0.003)	(0.188)	(0.817)	
Y24	1.944	0.598	1.004	1.838	7.688	0.001
	(0.036)	(0.055)	(0.003)	(0.136)	(0.931)	
Y30	1.988	0.609	1.003	1.809	7.330	0.001
	(0.037)	(0.056)	(0.003)	(0.132)	(0.891)	
Y36	2.078	0.610	1.003	1.680	6.641	0.001
	(0.037)	(0.053)	(0.003)	(0.127)	(0.762)	
Y48	2.146	0.602	1.003	1.673	6.589	0.001
	(0.036)	(0.051)	(0.003)	(0.130)	(0.765)	
Y60	2.285	0.586	1.003	1.476	5.841	0.001
	(0.035)	(0.045)	(0.003)	(0.130)	(0.631)	

주: 1) ( )안은 표준오차를, Y뒤의 숫자는 개월 수를 각각 의미한다.

<표 3> AA0 등급 회사채 수익률 기초 통계량[1)]

(단위: %)

만기	평균	표준편차	자기상관	왜도	첨도	Jarque-Bera Test(p-value)
Y12	1.807	0.526	1.005	1.601	8.263	0.001
	(0.032)	(0.045)	(0.003)	(0.191)	(0.812)	
Y24	1.986	0.595	1.004	1.804	7.592	0.001
	(0.036)	(0.054)	(0.003)	(0.136)	(0.905)	
Y30	2.029	0.605	1.003	1.784	7.280	0.001
	(0.037)	(0.055)	(0.003)	(0.132)	(0.875)	
Y36	2.119	0.607	1.003	1.663	6.594	0.001
	(0.037)	(0.052)	(0.003)	(0.126)	(0.752)	
Y48	2.195	0.600	1.003	1.635	6.468	0.001
	(0.036)	(0.050)	(0.003)	(0.129)	(0.740)	
Y60	2.351	0.586	1.002	1.449	5.753	0.001
	(0.035)	(0.044)	(0.003)	(0.131)	(0.614)	

주: 1) ( )안은 표준오차를, Y뒤의 숫자는 개월 수를 각각 의미한다.

<표 4> AA- 등급 회사채 수익률 기초 통계량[1)]

(단위: %)

만기	평균	표준편차	자기상관	왜도	첨도	Jarque-Bera Test(p-value)
Y12	1.845	0.518	1.005	1.613	8.305	0.001
	(0.031)	(0.043)	(0.003)	(0.191)	(0.813)	
Y24	2.033	0.590	1.004	1.867	7.769	0.001
	(0.036)	(0.054)	(0.003)	(0.136)	(0.947)	
Y30	2.077	0.603	1.003	1.823	7.367	0.001
	(0.036)	(0.055)	(0.003)	(0.132)	(0.895)	
Y36	2.162	0.607	1.003	1.693	6.667	0.001
	(0.037)	(0.052)	(0.003)	(0.126)	(0.764)	
Y48	2.270	0.597	1.003	1.602	6.359	0.001
	(0.036)	(0.049)	(0.003)	(0.129)	(0.717)	
Y60	2.460	0.581	1.002	1.421	5.630	0.001
	(0.035)	(0.043)	(0.003)	(0.131)	(0.599)	

주: 1) ( )안은 표준오차를, Y뒤의 숫자는 개월 수를 각각 의미한다.

자료의 구조를 자세히 알아보기 위해 아래에서는 주성분 분석(PCA)을 수행하였다. 각 채권의 공분산행렬에 대해 특성근 분해(eigenvalue decom- position)를 수행함으로써 주성분 요인과 요인별 기여도를 산출할 수 있다. 아래 [그림 2]에서 보면 채권별 주성분 분석에서 1요인인 수준(level)의 경우에는 대체로 유사한 모습을 보이는 반면 2요인인 기울기(slope)에서는 국고채와 회사채 간에는 명확한 차이를 가진 것이 확인되며 회사채 내에서는 신용등급에 관계 없이 대체로 유사한 모습을 가지는 것으로 나타났다. 이러한 결과는 국고채와 회사채의 수익률 구조를 동시에 추정할 경우 수익률 구조에서 기울기를 설명하는 모수가 유의하게 나타날 것임을 시사한다.

[그림 2] 채권별 주성분 분석 결과

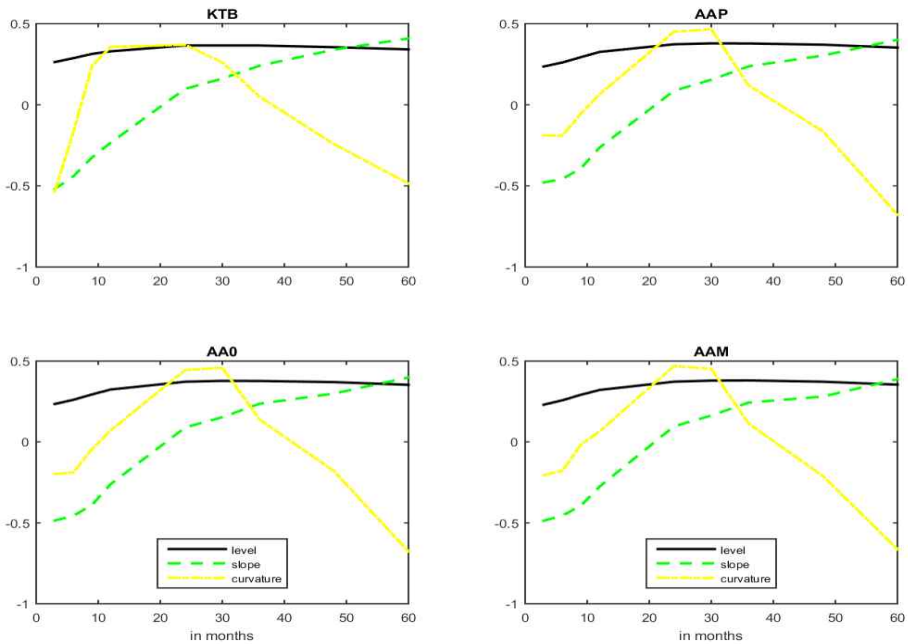

주성분 분석에서 도출한 3가지 요인의 시계열을 살펴보면 [그림 3]과 같은데 이자율 동학은 대부분 수준 요인에 의해 주도되고 있어 기울기와 곡률 요인의 변화는 거의 나타나지 않고 있음을 알 수 있다. 특히 기울기와 곡률 요인의 움직임이 유사하게 분석되고 있어 이 두 요인을 모두 고려하여 모형을 설정할 실익이 높

지 않고 분석 기간 동안 이자율의 만기별 구조는 상당히 편평한 모습을 가지고 있음을 간접적으로 파악할 수 있다.

[그림 3] 주성분 요인의 시계열 추이

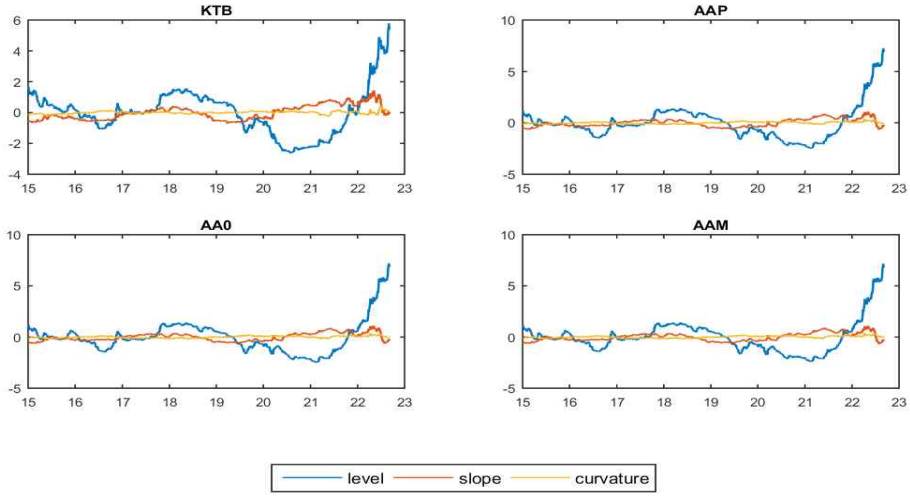

주성분 요인의 시계열 추이에서 살펴본 정성적인 결과를 보다 정량화하여 요인 개수의 선택을 결정하기 위해서 주성분 분석의 요인별 누적 기여도를 살펴볼 필요가 있는데 분석 결과는 <표 5>에 제시되어 있다. 그 결과 채권별로 2요인까지만 고려하더라도 채권 수익률의 변동의 99% 이상을 설명하는 것으로 나타나 두 개의 요인만을 고려해도 충분할 것으로 해석된다. 따라서 신용위험을 감안한 이자율 기간구조 모형을 설정하기 위해서는 채권별로 2요인이 필요하고 국고채와 회사채 간의 신용도 차이를 반영하는 요인이 추가적으로 필요하므로 3요인을 고려한 선형 이자율모형으로도 이자율 구조를 충분히 반영할 수 있을 것으로 사료된다.

<표 5> 주성분 분석의 요인 누적 기여도

(단위: %)

요인	KTB	AA+	AA0	AA-
1	0.9027	0.9421	0.9415	0.9408
1+2	0.9952	0.9945	0.9944	0.9942
1+2+3	0.9980	0.9980	0.9980	0.9980

2. 추정 결과

국고채와 AA+와의 금리 차이가 크지 않아 상태변수의 식별이 용이하도록 하기 위해 모수 추정에서는 국고채와 AA-등급 회사채 자료를 사용하였다. <표 6>에서는 3요인 선형 이자율모형의 모수를 추정한 결과를 제시하였다. 대부분의 모수 추정값이 통계적으로 유의한 수준을 보였으나 상태변수 모수인 κ_{11}, κ_{31}, κ_{33} 및 위험의 시장가격 모수인 λ_{11}의 경우는 통계적인 유의성을 가지지 못하는 것으로 나타났다. 위험의 시장가격 모수에서 λ_{02}가 다른 모수에 비해 큰 값을 보이는 것으로 나타났는데 이는 두 번째 상태변수가 이자율기간구조에서 기울기를 조절하게 되는데 2015년 이후 장기간 이어진 저금리로 만기별 이자율 변화가 크지 않기 때문에 발생한 것으로 보인다.

<표 6> 3요인 선형 이자율기간구조 모형 추정 결과

변수		모수	추정치	표준오차	p-value
무위험 이자율	$r(t)$	a_0	0.2055	0.0345	0.0000
		a_1	0.0096	0.0012	0.0000
		a_2	0.0086	0.0007	0.0000
위험 이자율	$R(t)$	b_0	-0.0408	0.0137	0.0032
		b_1	0.9044	0.0302	0.0000
		b_2	0.0023	0.0002	0.0000
상태 변수	$X(t)$	κ_{11}	0.0411	0.0486	0.3985
		κ_{21}	5.2857	0.4679	0.0000
		κ_{22}	1.3897	0.3453	0.0001
		κ_{31}	0.6942	0.3352	0.0391
		κ_{32}	0.2527	0.1588	0.1124
		κ_{33}	0.0969	0.0913	0.2893
위험의 시장 가격	$\lambda(t)$	λ_{01}	-0.5213	0.2564	0.0428
		λ_{02}	34.7936	0.6711	0.0000
		λ_{03}	-5.7180	0.2938	0.0000
		λ_{11}	0.0154	0.0485	0.7510
		λ_{22}	1.2012	0.3373	0.0004
		λ_{33}	0.2423	0.0907	0.0079

3요인 선형이자율 모형에 의한 추정 결과를 바탕으로 추정한 국고채와 회사채의 초단기이자율의 시계열 추이 및 초단기이자율 스프레드를 [그림 4]에 도시하였다. 무위험채와 신용채 간의 초단기이자율 스프레드는 대체로 2020년 이후를 기점으로 확대되는 양상을 보이고 있으며 최근에는 스프레드가 1%p 정도 수준인 것으로 분석되었다. 이러한 스프레드의 차이는 신용 위험에 기반한 것으로 2020년 이후의 유동성 압박이 신용 위험으로 전이되고 있음을 시사한다.

[그림 4] 국고채 및 회사채(AA-) 초단기이자율의 시계열 및 스프레드 추이

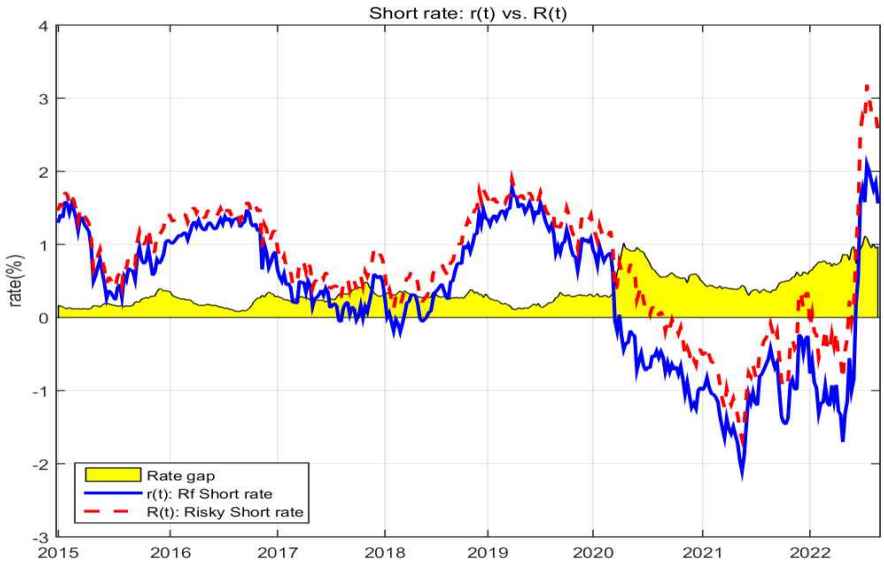

한편 국고채와 회사채의 초단기이자율과 연립상미분방정식을 풀어 도출한 $c(n)$과 $d(n)$을 이용하여 3년물 및 5년물 무위험채권 및 신용채의 수익률과 실제 데이터를 비교한 결과를 [그림 5]와 [그림 6]에 도시하였다. 각 만기별로 추정 모수를 이용한 추정 수익률과 실제 수익률이 유사한 패턴을 보이고 있어 추정 작업은 대체로 적절히 수행된 것으로 판단된다. 추정 작업의 정밀도를 확인하기 위해서 표본 내 적합도와 표본 외 예측력을 살펴보는 작업을 수행하는 것도 의미가 있지만 본고의 목적이 어떤 모형의 예측력이 높은지를 평가하는 것이 아니라 이자율 기간구조를 분해하고 통화정책의 효과성을 살펴보는 것이므로 대표적인 만기에 대한 실제 및 추정 현물이자율을 비교하는 것으로 모형의 설명력을 대신하고자 한다.

[그림 Ⅲ-5] 3년 만기 국고채 및 회사채 실제 현물이자율과 추정 현물이자율

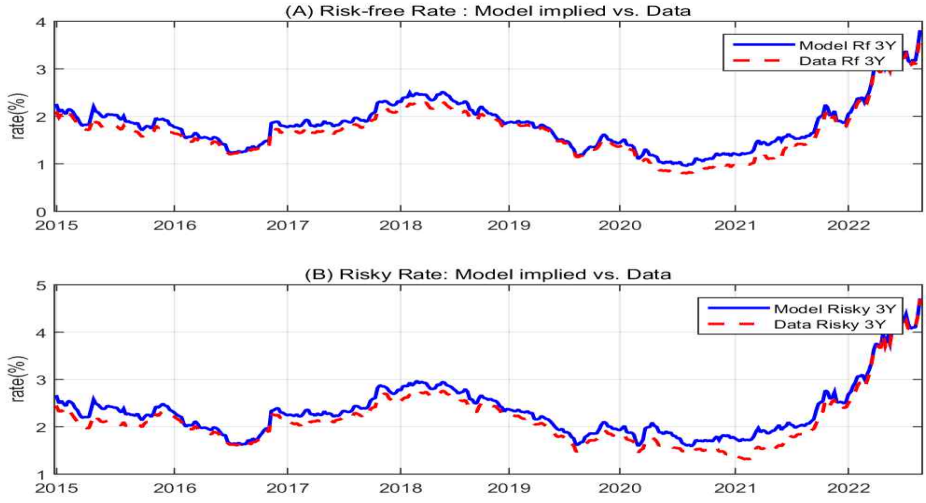

[그림 Ⅲ-6] 5년 만기 국고채 및 회사채 실제 현물이자율과 추정 현물이자율

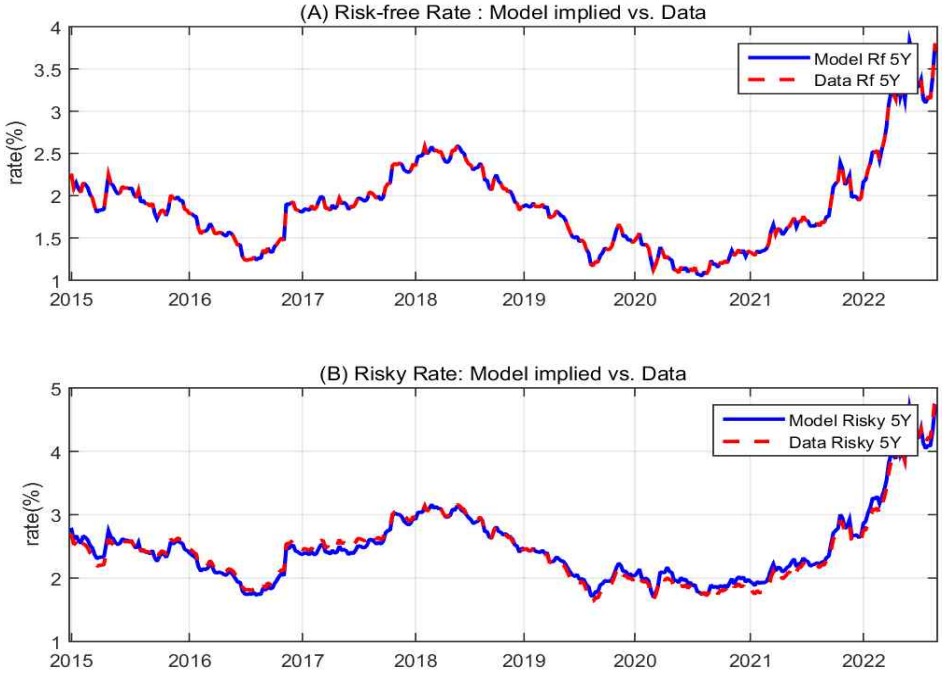

분석에 사용된 자료를 기준으로 동일 만기의 신용채와 무위험채의 이자율 스프레드(=$r_{회사채}(n) - r_{국고채}(n)$)를 살펴보면 <표 7>에서는 만기에 따라 스프레드의 평균은 (0.39%, 0.60%)의 범위를 가지고 있으며 높은 자기상관성과 우측 편포 및 높은 첨도를 가지고 있음을 알 수 있다.

<표 7> 만기별 신용채 금리 스프레드 분석: 추정 자료[1)]

(단위: %)

만기	평균	표준편차	자기상관	왜도	첨도
Y12	0.3931	0.1695	0.9965	1.6022	5.1688
	(0.0223)	(0.0074)	(0.0200)	(0.2984)	(1.3795)
Y24	0.4529	0.1426	0.9974	1.6964	5.5753
	(0.0187)	(0.0055)	(0.0210)	(0.3125)	(1.5256)
Y30	0.4820	0.1323	0.9979	1.7220	5.6904
	(0.0174)	(0.0048)	(0.0212)	(0.3179)	(1.5731)
Y36	0.5090	0.1233	0.9984	1.7421	5.7821
	(0.0162)	(0.0042)	(0.0212)	(0.3228)	(1.6136)
Y48	0.5567	0.1082	0.9995	1.7739	5.9332
	(0.0142)	(0.0033)	(0.0211)	(0.3319)	(1.6830)
Y60	0.5963	0.0962	1.0006	1.8002	6.0668
	(0.0126)	(0.0026)	(0.0209)	(0.3400)	(1.7430)

주: 1) ( )안은 표준오차를, Y뒤의 숫자는 개월 수를 각각 의미한다.

Ⅳ. 기간프리미엄 추정 및 분석

여기서는 3장에서 추정된 결과를 바탕으로 기간프리미엄과 선도금리 기간프리미엄을 각각 도출하고자 한다. 다수의 선행 연구에서 기간프리미엄은 실물경기 역행성을 가지고 있는 것으로 주장하고 있으므로 본고에서는 이러한 연구 결과를 바탕으로 높은 기간프리미엄이 경기 불황을 예고하는 지표로 인식하고 분석을 수행한다.[4)]

4) 윤재호(2020)에서는 기간프리미엄이 24개월 이후의 산업생산 증가율과 생산갭의 예측에 유의한 예측력을 가지는 반면 소비자물가 상승률의 예측에는 유의하지 않는 예측력을 보였다고 설명한다.

아래 [그림 7-8]은 3년 만기 무위험채와 신용채를 대상으로 (무이표채) 현물이자율, 기대 단기이자율과 두 가지 형태의 기간프리미엄을 도시한 것이다. 두 그림 모두에서 관찰되는 특징은 2021년 이후 기대 단기이자율을 상승하는 반면 기간프리미엄은 하락하는 양상이 관찰됨을 알 수 있다. 기간프리미엄이 24개월의 예측 시계로 경기 역행적인 예측력을 가지고 있음을 감안할 때 2023년 정도에는 경기가 상승 국면으로 반전할 것임을 채권시장에서는 예측하고 있음을 알 수 있다. 기대 단기이자율의 경우는 2021년 이후 지속적인 상승세를 나타내고 있는데 단기이자율이 중앙은행의 정책금리에 영향을 받는 부분이 크다는 점을 감안하며 시장에서는 중앙은행의 정책금리 인상이 당분간은 지속적으로 이어질 것임을 예상하고 있음을 알 수 있다. 따라서 2021년 이후 관찰되는 금리 상승은 유동성이나 인플레이션 위험에 대한 보상으로서의 기간프리미엄보다는 정책금리 인상에 대한 예상을 반영한 것으로 해석된다.[5)]

이러한 결과의 강건성을 살펴보기 위해 [그림 9-10]에서는 5년 만기 무위험채와 신용채를 대상으로 현물이자율, 기대 단기이자율 및 기간프리미엄을 분석해 보았다. 구체적인 금리 수준을 제외하고 각 시계열들의 변화하는 양상을 보면 대체로 3년 만기물과 유사한 행태를 보이고 있음이 관찰된다. 이러한 결과는 최근의 금리 상승은 경기 불황에 대한 우려보다는 중앙은행 정책금리 인상에 의해 주로 견인된 것임을 시사한다.

5) 최근 유동성 위기를 전면에 부각시킨 강원도 레고랜드 사태는 2022년 9월 28일에 발생하여 분석 자료에는 이 기간이 포함되지 않았다.

[그림 7] 3년 만기 무위험채의 현물이자율, 기대 단기이자율 및 기간프리미엄

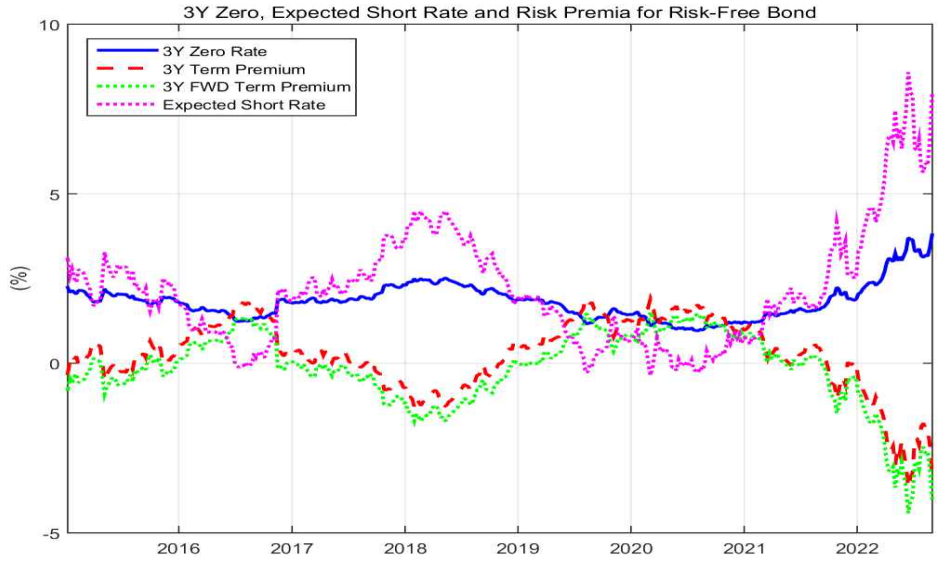

[그림 8] 3년 만기 신용채의 현물이자율, 기대 단기이자율 및 기간프리미엄

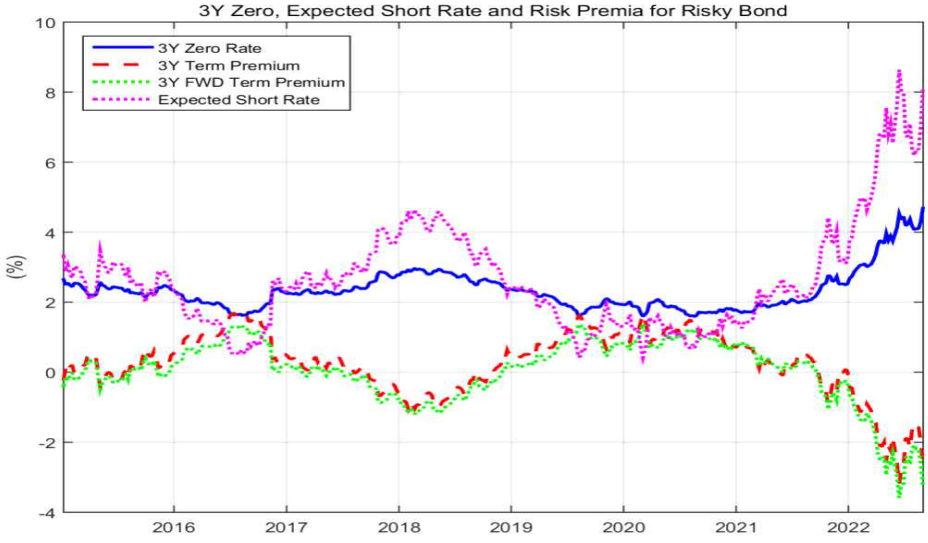

[그림 9] 5년 만기 무위험채의 현물이자율, 기대 단기이자율 및 기간프리미엄

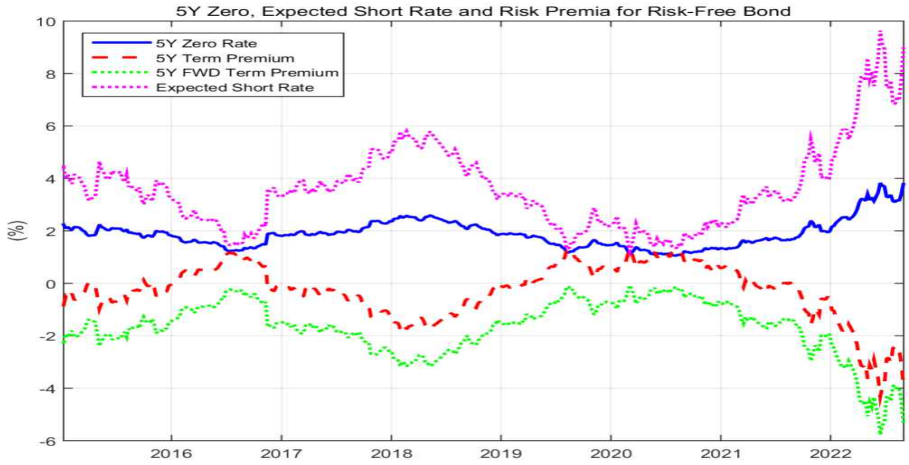

[그림 10] 5년 만기 신용채의 현물이자율, 기대 단기이자율 및 기간프리미엄

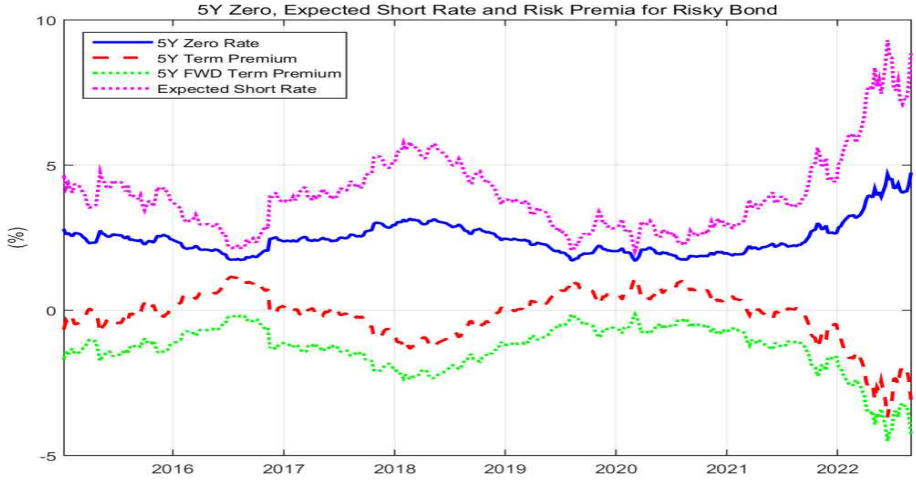

Ⅴ. 정책금리 변경의 효과 분석

여기서는 우리나라 중앙은행의 정책금리 변경의 효과성에 대해 살펴보고자 한다. 여기서 설명하는 효과성이란 정책금리의 변경이 단기이자율을 통해 수익률곡선을 변화시킴으로써 장기이자율의 변화를 야기하였는지를 평가하는 것이다.

한국은행의 기준금리는 2015년 3월 12일 종전의 2.0%에서 25bp 인하된 이후 2022년 7월 13일까지 총 15차례의 금리 변동을 경험하였다.[6] 특히 기준금리는 2021년 8월 26일에 이전보다 25bp 인상되어 0.75%를 기록한 이후 5차례에 걸쳐 지속적인 인상되어 왔으며 2022년 7월 13일에는 빅스텝(50bp) 인상을 통해 최종적으로는 2.25%에 이르렀다.

<표 8> 한국은행 기준금리 추이(2022. 8. 24일 현재)

연도	월/일	기준금리 (%)
2015	3/12	1.75
	6/11	1.50
2016	6/9	1.25
2017	11/30	1.50
2018	11/30	1.75
2019	7/18	1.50
	10/16	1.25
2020	3/17	0.75
	5/28	0.50
2021	8/26	0.75
	11/25	1.00
2022	1/14	1.25
	4/14	1.50
	5/26	1.75
	7/13	2.25

주 : 음영 부분은 기준금리 인하 시점
자료: 한국은행

[그림 11] 한국은행 기준금리

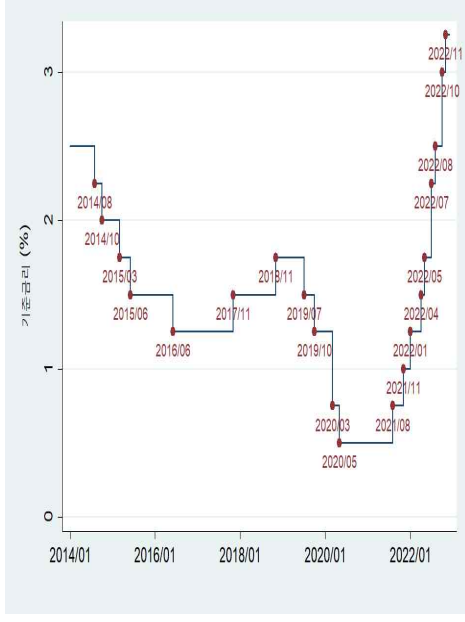

자료: 한국은행

6) 한국은행은 이후에도 기준금리를 지속적으로 인상해 왔으나 본고에서는 분석 자료 기간에 한정하여 기준금리 변동을 인식하고 있다는 점을 주지하기 바란다.

[그림 11]은 기준금리 인하 시점을 기준으로 전후 10일에 걸친 3년 만기 현물이자율, 기대 단기이자율 및 기간프리미엄의 누적 증분을, [그림 12]는 기준금리 인상 시점을 기준으로 전후 10일에 걸쳐 동일한 변수를 대상으로 누적 증분을 분석한 사건 연구(event study)의 결과이다.

두 사건 연구 결과에서 모두 기준금리의 인하 및 인상 시기에서 기대 단기이자율은 3년 현물이자율과 동일한 방향으로 움직이고 있음이 관찰된다. 기대 단기이자율은 선도이자율과 유사하게 현물이자율보다 높은 진폭을 보이고 있는데 이는 단기이자율이 한계이자율(marginal rate of interest)의 특성을 가지고 있는 반면 현물이자율은 평균이자율(average rate of interest)의 특성을 보이고 있기 때문이다.

최근의 금리 인상 시기를 기준으로 기대 단기이자율과 기간프리미엄의 움직임에서 살펴보면 몇가지 특이한 사항이 관찰된다. 먼저 자료상 가장 최근의 금리 인상 시기인 2022년 7월 13일의 경우에는 3년 만기 현물이자율의 누적 증분은 오히려 하락하고 있다는 점이다. 이러한 현상은 인플레이션 억제를 위한 중앙은행의 정책 기조와 중기적 시계에서의 부정적인 성장 전망을 시장에서 이미 예상하고 3년물 금리에 이러한 예상이 선반영되었기 때문인 것으로 판단된다. (결과 분석은 아직 미완성인 상태로 좀 더 추가해서 발표하도록 하겠습니다.)

[그림 12] 기준금리 인하 전후의 3년 만기 현물이자율, 기대 단기이자율 및 기간프리미엄의 누적 증분

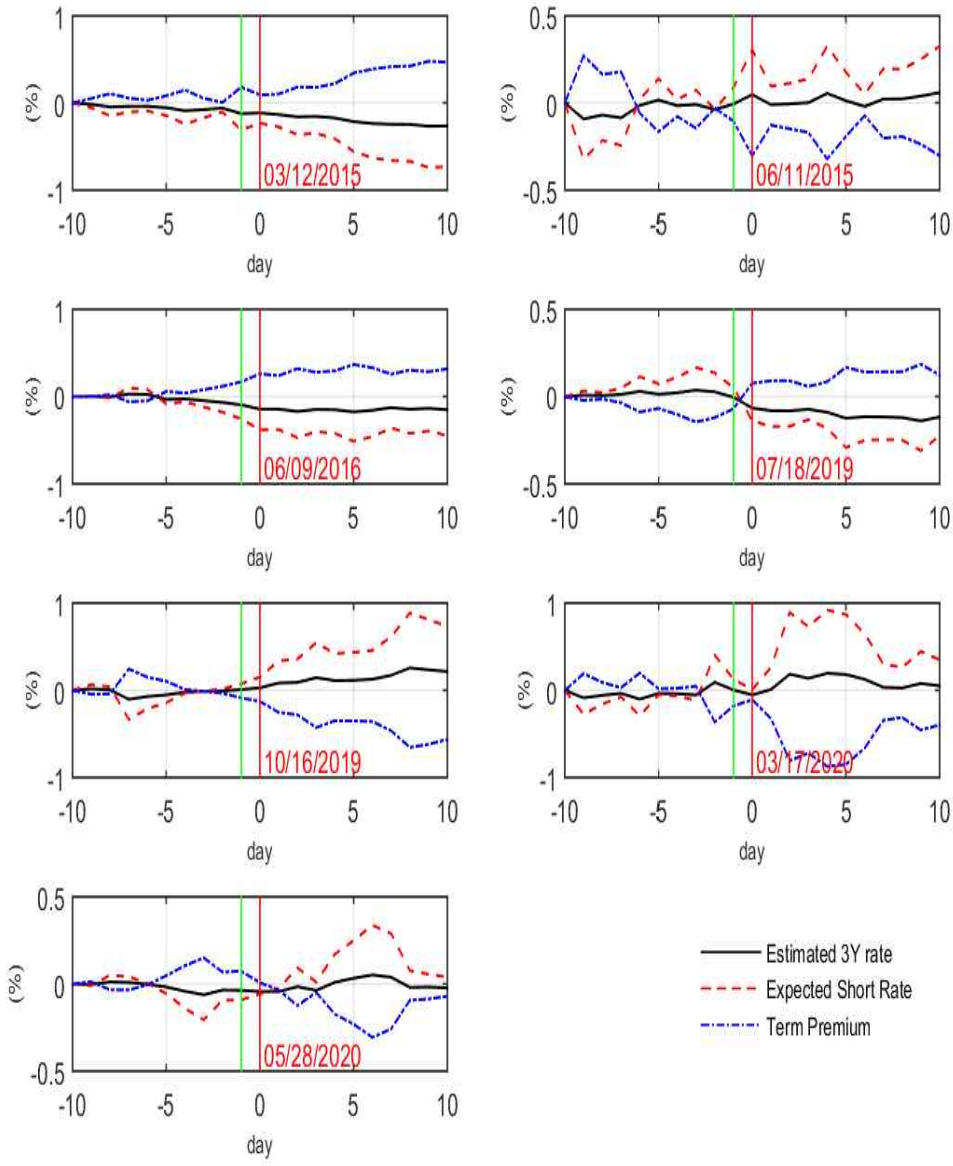

[그림 13] 기준금리 인상 전후의 3년 만기 현물이자율, 기대 단기이자율 및 기간프리미엄의 누적 증분

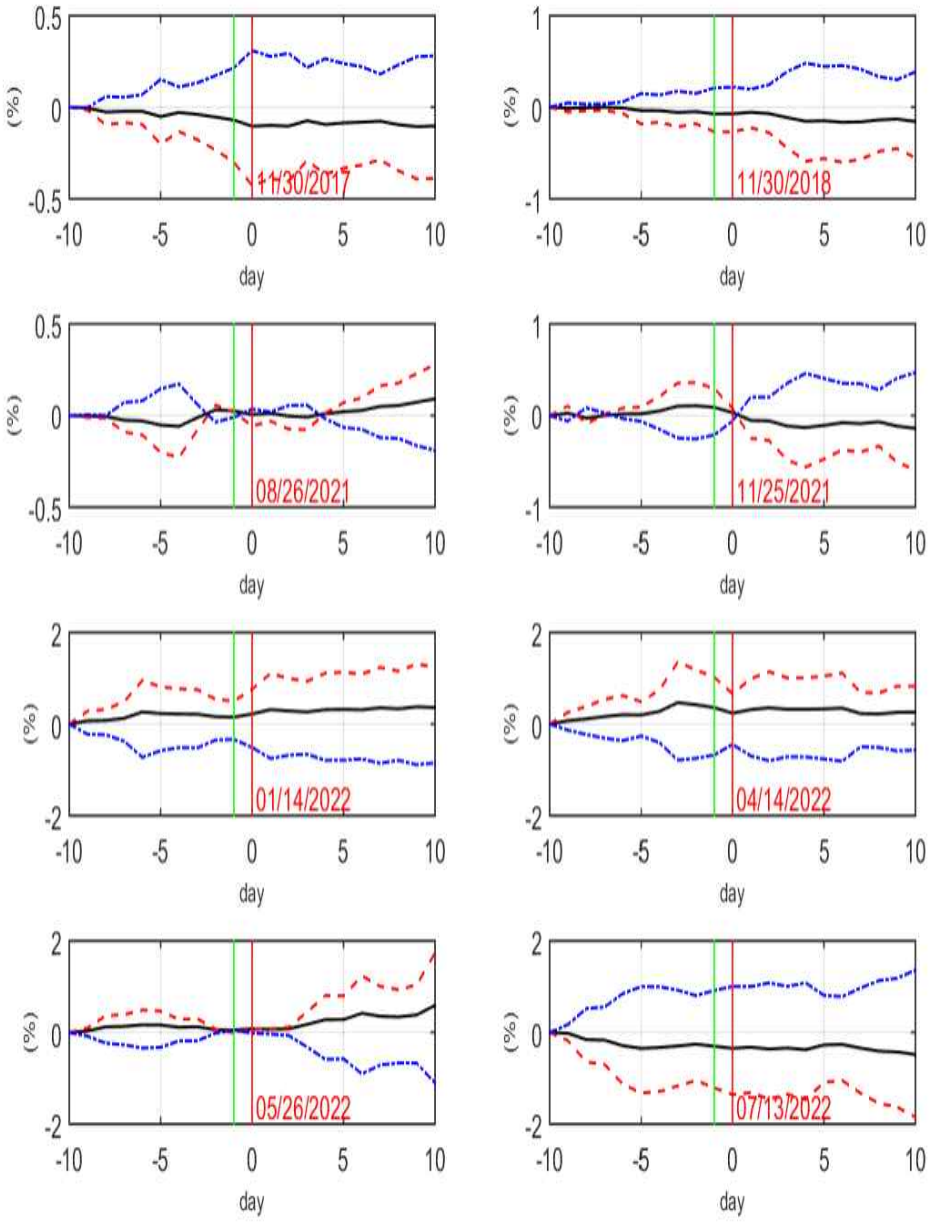

V. 결 론

TBA

참 고 문 헌

송준혁, “이자율 기간구조를 이용한 정책금리 변경의 효과 분석”, 한국개발연구 31(2), 2009, 14-45.

윤재호, “이자율 스프레드의 경기 예측력: 문헌 서베이 및 한국의 사례 분석”, 경제분석 26(3), 2020, 1-47.

Durham, J. Benson, “An Estimation of the Inflation Risk Premium Using a Three-Factor Affine Term Strructure Model”, Federal Reserve Board Finance and Economics Discussion Series 42, 2006.

Gurkaynak, R. S., and J. H. Wright, “Macroeconomics and the Term Structure”, Journal of Economic Literature 50(2), 2012, 331-367.

Kim, Don H., and Jonathan H. Wright, “An Arbitrage-Free Three-Factor Term Structure Model and the Recent Behavior of Long-Term Yields and Distant-Horizon Forward Rates”, Federal Reserve Board Finance and Economics Discussion Series 33, 2005.

Kim, Don H., and Athanasios Orphanides, “Term Structure Estimation with Survey Data on Interest Rate Forecasts”, Federal Reserve Board Finance and Economics Discussion Series 48, 2005.

Ludvigson, S., and S. Ng, “Macro Factors in Bond Risk Premia” Review of Financial Studies, 22, 2009, 5027-5067.

Rudebusch. G. D., and B. P. Sack, and E. T. Swanson, “Macroeconomic Implications of Changes in the Term Premium”, Federal Reserve Bank of St. Louis Review 84, 2007. 242-269.

Annals of Operations Research
https://doi.org/10.1007/s10479-022-04900-3

ORIGINAL RESEARCH

Identifying household finance heterogeneity via deep clustering

Yoontae Hwang[1] · **Yongjae Lee**[1] · **Frank J. Fabozzi**[2]

Accepted: 28 July 2022

Abstract
Households are becoming increasingly heterogeneous. While previous studies have revealed many important insights (e.g., wealth effect, income effect), they could only incorporate two or three variables at a time. However, in order to have a more detailed understanding of complex household heterogeneity, more variables should be considered simultaneously. In this study, we argue that advanced clustering techniques can be useful for investigating high-dimensional household heterogeneity. A deep learning-based clustering method is used to effectively handle the high-dimensional balance sheet data of approximately 50,000 households. The employment of appropriate dimension-reduction techniques is the key to incorporate the full joint distribution of high-dimensional data in the clustering step. Our study suggests that various variables should be used together to explain household heterogeneity. Asset variables are found to be crucial for understanding heterogeneity within wealthy households, while debt variables are more important for those households that are not wealthy. In addition, relationships with sociodemographic variables (e.g., age, education, and family size) were further analyzed. Although clusters are found only based on financial variables, they are shown to be closely related to most sociodemographic variables.

Keywords Household finance · Heterogeneous household · High-dimensional data · Clustering · Machine learning · Deep learning

1 Introduction

Households are becoming increasingly heterogeneous, due to increasing wealth inequalities (Atkinson et al., 2011; Piketty, 2013), financial crisis (Krueger & Perri, 2006), or the COVID-19 pandemic (Blundell et al., 2020; Dizioli & Pinheiro, 2021). Krueger et al. (2016) found

✉ Yongjae Lee
yongjaelee@unist.ac.kr

✉ Frank J. Fabozzi
fabozzi321@aol.com

[1] Department of Industrial Engineering, Ulsan National Institute of Science and Technology (UNIST), 50 UNIST gil, Ulju gun, Ulsan 44919, Republic of Korea

[2] EDHEC Business School, 393 Promenade des Anglais, 06202 Nice Cedex 3, France

Published online: 21 September 2022

that households in different segments of the wealth distribution had different reactions to the 2007–2008 Global Financial Crisis, and Eichenbaum et al. (2021) reported that households have different COVID-19 pandemic mortality rates depending on their income levels. Consequently, many researchers have investigated the heterogeneity of household finances in various aspects. For example, heterogeneity in portfolio composition (Mankiw & Zeldes, 1991; Heaton & Lucas, 1997; Krusell & Smith, 1997; Case et al., 2005, 2011), income level (Constantinides & Duffie, 1996; Krueger et al., 2016; Lucas, 1994; Ahn et al., 2018), wealth level (Bricker et al., 2021; Case et al., 2005, 2011; Krueger et al., 2016), and demographics (Campbell, 2006; Berton et al., 2018; Calvet et al., 2021; Das et al., 2020) have been identified and analyzed.

However, Jappelli and Pistaferri (2014) and Krueger et al. (2016) pointed out the limitations of existing studies that separately investigate household heterogeneity in each dimension (e.g., income and wealth). That is, considering a few variables would not be enough to have a more detailed understanding of complex household heterogeneity. Krueger et al., (2016, p. 67) further noted that additional dimensions of household heterogeneity should be introduced to "better capture the joint distribution of wealth, income, and expenditure we observe in the data."

Figure 1 illustrates the average asset allocation of Korean households with respect to their wealth percentile from 2017 to 2020. Panel a of Fig. 1shows the results for the entire dataset. The proportions of deposit savings and long-term rental deposits almost monotonically decrease as households become wealthier. The proportion of residential housing increases up to middle class households, but it suddenly decreases. Instead, the proportion of nonresidential real estate increases. It is clear that the relationship between households' asset allocation and wealth level is nonlinear. Panels b and c of Fig. 1 represent the results from the bottom 20% and the top 20% income households, respectively. The relationship is clearly not simplified even if we look at subgroups partitioned by income level. This shows why conventional approaches would have difficulties in investigating the heterogeneity in household finance, which involves nonlinear relationships that are entangled in a multi-dimensional space.

Consequently, in this study, we perform a comprehensive analysis of household finance heterogeneity in various dimensions using an advanced clustering method. Since household wealth, income, and consumption are known to have skewed marginal distributions (Campbell, 2006), it would be difficult to fit such data using standard probability distributions. We believe that clustering methods can be helpful because these methods are specifically

Fig. 1 Average portfolio weights of Korean households in 2017–2020

designed to find representative clusters based on the multidimensional joint distribution of data points. Because household financial data would have a complex dependence structure between a large number of items, deep learning-based and manifold learning-based dimension reduction techniques are employed along with conventional clustering methods. Many studies have shown that deep learning and manifold learning methods are helpful for handling complex nonlinear dependent structures (Bengio et al., 2012).

While we use only the financial aspects (as reported in the balance sheets) of households to identify the representative clusters, the clusters are analyzed in terms of multiple criteria. That is, the clusters are analyzed in terms of household demographics (age, gender, education, family size, and employment) as well as households' balance sheets (income, expenditure, assets, and debt). Our analysis shows that financial heterogeneity is closely related to demographic heterogeneity.

Korean household finance and living condition survey data were used in this study. Annual data from 2017 to 2019 consist of balance sheets (including income, expenditure, assets, and debt) and demographics (including age, gender, education, and employment status of householder, family size) of around 20,000 households each year. The Republic of Korea has shown remarkable growth since the Korean War in the 1950s to become the world's 10th largest economy in 2020 according to the World Bank (2021). However, such rapid growth has been accompanied by various social issues. Currently, Korea has the world's lowest fertility rate (OECD, 2021) and severe inter- and intra-generational wealth inequality compared to other developed countries (OECD, 2018). Hence, Korea offers a good example of a clearer heterogeneity in household finance.

The remainder of this paper is organized as follows. Section 2 introduces the clustering method employed in this study, Sect. 3 discusses the data and experimental setting, and Sect. 4 presents findings from the numerical experiments. Finally, Sect. 5 concludes the study.

2 Deep clustering

Consider a household i's balance sheet data $\boldsymbol{x^i} \in \mathbb{R}^d$, which consists of asset variables $\boldsymbol{x^i_A} \in \mathbb{R}^{d_A}$, debt variables $\boldsymbol{x^i_D} \in \mathbb{R}^{d_D}$, and expenditure variables $\boldsymbol{x^i_E} \in \mathbb{R}^{d_E}$. Hence, $\boldsymbol{x^i} = [\boldsymbol{x^i_A}; \boldsymbol{x^i_D}; \boldsymbol{x^i_E}] \in \mathbb{R}^d$. Our purpose is to find k clusters that divide N households based on their balance sheet data $\boldsymbol{X} \in \mathbb{R}^{N \times d}$ so that each cluster would contain households that are similar in terms of their financial status. Hence, we apply clustering algorithms to households' balance sheet data $\mathbf{X} \in \mathbb{R}^{N \times d}$.

Clustering is one of the most popular unsupervised machine learning tasks that clusters through the similarity of data points without any label information (i.e., uses an unlabeled data). The objective of clustering is to maximize intra-group similarities and minimize inter-group similarities. Clustering methods have been shown to be useful in various tasks, such as images, medical, and finance (Ahmad & Khan, 2019).

The well-known clustering methods such as k-means, DBSCAN, hierarchical clustering, and Gaussian mixture model (GMM) have been successfully employed in various fields.[1] However, such conventional methods are not suitable for handling high-dimensional data.

Recently, many studies have shown that deep learning methods can be useful for enhancing clustering methods to effectively handle high-dimensional datasets. The so-called "deep clustering" methods have been proposed. Ghasedi Dizaji et al. (2017) and Caron et al.

[1] Saxena et al. (2017) and Ahmed and Khan (2019) provide a comprehensive review of conventional clustering algorithms.

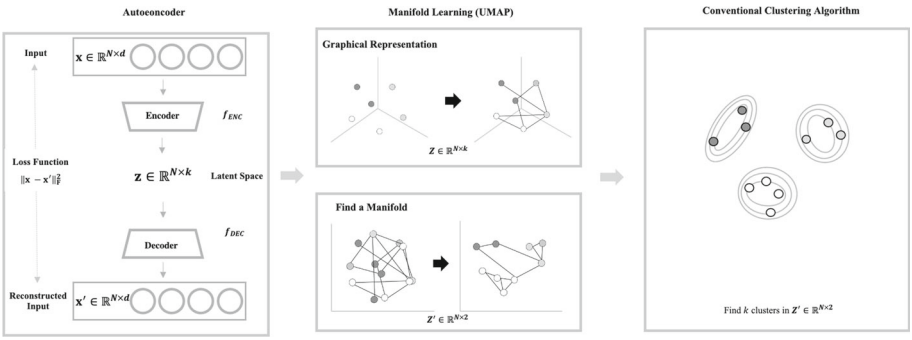

Fig. 2 N2D framework for deep clustering by McConville et al. (2021) (Created by the authors)

(2018) proposed clustering neural network models that utilize extracted important features from high-dimensional image data using a convolution neural network and an autoencoder,[2] respectively, which are jointly learned by interacting with conventional clustering methods (e.g., k-means). Guo et al. (2017) and Mukherjee et al. (2019) proposed clustering methods based on latent modeling using an autoencoder and generative adversarial networks,[3] respectively, and tested them on tabular data and image data. However, there was no significant performance improvement compared to conventional clustering methods.

McConville et al. (2021) proposed a simple deep clustering framework called N2D that directly uses conventional clustering algorithms (e.g., GMM) in a latent space found by deep learning and manifold learning techniques (see Fig. 2). Unlike other deep clustering methods mentioned earlier, the clustering step is separated from the dimension-reduction step. The N2D approach has been shown to achieve similar or even better performance compared to other deep clustering methods as well as conventional approaches. The key trick was to combine deep learning and manifold learning techniques to reduce the dimensionality of data by capturing complex nonlinear dependency structures. Therefore, we follow the N2D framework proposed by McConville et al. (2021) to find representative clusters of household balance sheet data.

For a household i's balance sheet data x^i, we first find its k-dimensional embedding $z^i \in \mathbb{R}^k$ via an autoencoder, and we further reduce it into a two-dimensional embedding $z'^i \in \mathbb{R}^2$ via UMAP. Then, clustering is performed with the two-dimensional embeddings z'^i of all households (i.e., for all i). The following subsections will explain in detail the two steps: (1) dimension reduction (autoencoder and UMAP) and (2) clustering (GMM).

[2] Convolutional neural networks refer to neural networks with specific structures that are known to be effective for handling image data (see Alzubaidi et al. (2021) for more detailed information). Autoencoders refer to a wide range of neural network models for dimension reduction tasks, and we will discuss these models further in Sect. 2.1.1.

[3] Generative adversarial networks (Goodfellow et al. 2014) are generative models that try to achieve high performance via adversarial training of two different neural networks. Xia et al. (2021) provides a summary of their variants and application examples.

2.1 Dimension reduction for clustering

Dimension reduction techniques are incorporated in most deep clustering methods to effectively handle high-dimensional data. The key to dimension reduction is to find low-dimensional representations (or features) lying in a high-dimensional space, which is often called latent modeling or feature extraction (Bengio et al., 2013). While other deep clustering algorithms jointly optimize latent modeling (or feature extraction) and clustering iteratively, McConville et al. (2021) separate the two tasks to simplify the overall process. However, to retain (or even improve) the performance of other deep clustering methods, they further divided the dimension reduction part into two. First, an autoencoder is used to find mid-dimensional embeddings to capture the global features. Second, manifold learning techniques, such as t-SNE and UMAP, are used to find low-dimensional manifolds to better capture local features. McConville et al. (2021) argue that such an approach can find more clusterable embeddings because both global and local features are crucial for clustering tasks.

2.1.1 Autoencoder

An autoencoder (AE) is a dimension reduction technique based on artificial neural networks and is often referred to as a deep learning version of principal component analysis (PCA), one of the most popular dimension reduction methods. While PCA is only able to capture linear dependence structures within data, AE is known to capture complex non-linear dependencies well (Bengio et al., 2013; Burges, 2010; Burges, 2010; Xie et al., 2016).

The AE is composed of an encoder function $f_{ENC} : \mathbb{R}^d \to \mathbb{R}^k$ and a decoder function $f_{DEC} : \mathbb{R}^d \to \mathbb{R}^k$. The encoder function f_{ENC} is a mapping from high-dimensional data $\mathbf{X} \in \mathbb{R}^{N\times d}$ with N samples and d features to corresponding embeddings $\mathbf{Z} \in \mathbb{R}^{N\times k}$ in a k-dimensional latent space with $k \ll d$. The decoder function f_{DEC} is a mapping from embeddings $\mathbf{Z} \in \mathbb{R}^{N\times k}$ to the original data $\mathbf{X} \in \mathbb{R}^{N\times d}$. AE is trained to minimize the following reconstruction loss:

$\ell_{\text{AE}} = \|\mathbf{X} - f_{DEC}(f_{ENC}(\mathbf{X}))\|_{\boldsymbol{F}}^2$,

where $\|\bullet\|_{\text{F}}^2$ is the Frobenius norm. While various neural network structures (e.g., convolutional neural networks and recurrent neural networks) can be used for both encoder and decoder functions, we use fully connected layers with a rectified linear unit (ReLU) for both functions. More details regarding the architectural choices are discussed in Appendix A.

Hence, the entire household balance sheet data $\mathbf{X} \in \mathbb{R}^{N\times d}$ is reduced to $\mathbf{Z} \in \mathbb{R}^{N\times k}$. Note that the embeddings are not separately found for asset, debt, and expenditure variables. Instead, each embedding incorporates all balance sheet variables so that the final clustering is done based on the entire balance sheet, not just subsets.

However, embeddings $\mathbf{Z} \in \mathbb{R}^{N\times k}$ found by AE do not necessarily preserve distances between data points $\mathbf{X} \in \mathbb{R}^{N\times d}$ in the original space, because AE is trained only in terms of minimizing the reconstruction loss. For any two data points $\mathbf{x_i}, \mathbf{x_j} \in \mathbb{R}^d$ and their autoencoded embeddings $\mathbf{z_i} = f_{ENC}(\mathbf{x_i}), \mathbf{z_j} = f_{ENC}(\mathbf{x_j}) \in \mathbb{R}^k$, there is no relationship between $d(\mathbf{x_i}, \mathbf{x_j})$ and $d(\mathbf{z_i}, \mathbf{z_j})$, where d is an arbitrary distance measure. Then, autoencoded embeddings would not be appropriate for clustering because the objective of clustering is to find similar data points.

Therefore, in the N2D framework, clustering is not performed on the auto-encoded embeddings. Instead, AE is used to find intermediate embeddings with its dimension k not being too small, so that the distances in the original space are not fully lost. McConville et al. (2021) recommend using the dimension of autoencoded embeddings k as the desired number of clusters.

2.1.2 UMAP: uniform manifold approximation and projection

The manifold assumption in machine learning is that the observed data lie approximately on a low-dimensional manifold, and manifold learning refers to non-linear dimension reduction techniques based on such an assumption. Because a manifold is a topological concept in which every point is locally connected, manifold learning techniques are known to capture local features well. Many different models have been proposed, including isometric mapping (Tenenbaum et al., 2000), locally linear embedding (Tenenbaum et al., 2000), modified locally linear embedding (Zhang & Wang, 2007), Hessian eigenmapping (Donoho & Grimes, 2003), and t-distributed stochastic neighbor embedding (Van der Maaten & Hinton, 2008). While the last one (t-SNE) showed promising performance for complex datasets, it is often criticized for being too locally focused and lacks scalability (McConville et al., 2021).

In this regard, uniform manifold approximation and projection (UMAP) was recently proposed by McInnes et al. (2018), which is known to preserve the global structure as well as the local structure of data through a cross-entropy cost function. Let us consider a dimension-reduction task from $\mathbf{Z} \in \mathbb{R}^{N\times k}$ to $\mathbf{Z}' \in \mathbb{R}^{N\times 2}$. In other words, we wish to reduce k-dimensional dataset into two-dimensional embeddings. UMAP consists of three steps. First, graph construction. In this step, a graphical representation of $\mathbf{Z} \in \mathbb{R}^{N\times k}$ is presented. The relationship between two data points $z_i, z_j \in \mathbb{R}^k$ is represented as a probability

$$\mathrm{p}_{i|j} = \exp\left(-\frac{d(z_i, z_j) - \rho_i}{\sigma_i}\right),$$

where d is a distance measure, ρ_i is a local connectivity parameter, and σ_i is a normalization factor. Here, ρ_i is set as the average distance from z_i to its u nearest neighbors, where u controls the balance between local and global structure. If u is low, the UMAP model would focus on more detailed local structure, while a high u would ignore small details to represent global structure. Then, the global probability between the two data points is computed as.

$$\mathrm{p}_{ij} = (\mathrm{p}_{i|j} + \mathrm{p}_{j|i}) - \mathrm{p}_{i|j}\mathrm{p}_{j|i}$$

Second, graph embedding. For the corresponding embeddings $z'_i, z'_j \in \mathbb{R}^2$, the pairwise probability q_{ij} is computed as:

$$q_{ij} = \frac{1}{1 + a\|z'_i - z'_j\|^{2b}},$$

where a and b are hyper-parameters, and $\| \bullet \|$ is a norm function. Finally, cross-entropy is used as a loss function to find the optimal mapping $f_{UMAP} : \mathbb{R}^k \to \mathbb{R}^2$ from $\mathbf{Z} \in \mathbb{R}^{N\times k}$ to $\mathbf{Z}' \in \mathbb{R}^{N\times 2}$ from a fuzzy topological point of view. The cross-entropy loss function can be expressed as follows:

$$\ell_{\mathrm{UMAP}} = \sum_{i\neq j} p_{ij}\log\left(\frac{p_{ij}}{q_{ij}}\right) + (1 - \mathrm{p}_{ij})\log\left(\frac{1 - p_{ij}}{1 - q_{ij}}\right)$$

McConville et al. (2021) tested various manifold learning techniques (isomapping, t-SNE, and UMAP) for their N2D framework, and N2D with UMAP demonstrated the best performance. Therefore, we use UMAP to find the final two-dimensional embeddings $\mathbf{Z}' \in \mathbb{R}^{N\times 2}$ from the intermediate embeddings $\mathbf{Z} \in \mathbb{R}^{N\times k}$ found by AE.

2.2 Clustering via Gaussian mixture model

Finally, the Gaussian mixture model (GMM) is employed to find clusters for the two-dimensional embeddings $\mathbf{Z}' \in \mathbb{R}^{N\times 2}$ found by AE and UMAP. Consider a k mixture of Gaussian distributions

$$\mathrm{p}(\mathrm{z}) = \sum_{i=1}^{k} \pi_i \mathcal{N}(\mathrm{z} \mid \mu_i, \Sigma_i),$$

where $\mathcal{N}(\mathrm{z} \mid \mu_i, \Sigma_i)$ is a multi-dimensional Gaussian distribution with mean μ_i and covariance matrix Σ_i, and π_i is a weight coefficient with $\pi_\mathrm{i} \geq 0$ and $\sum_{i=1}^{k} \pi_i = 1$. GMM finds the optimal parameters of the above Gaussian mixture that are most likely for the given data. That is, a log-likelihood given parameter θ_{GMM}

$$\ell_{\mathrm{GMM}} = \ln \mathrm{p}\left(\mathbf{Z}' \mid \theta_{\mathrm{GMM}}\right) = \sum_{j=1}^{N} \ln \left\{ \sum_{i=1}^{k} \pi_i \mathcal{N}\left(\mathrm{z}'_j | \mu_i, \Sigma_i\right) \right\}$$

is maximized with respect to θ_{GMM}. Subsequently, the resulting k Gaussian distributions were considered as the optimal clusters.

Of course, conventional clustering methods would be subject to robustness issues with respect to initial points. Since k-means or GMM all start from random initial points and are not always guaranteed to converge to global optima, such clustering algorithms are often built to run multiple times with different random initial points and select the best one among them. We also use the same method to obtain more robust results.

3 Data and model

In this section, we describe our data and models (Sect. 3.1), and a simple analysis was performed to determine the appropriate number of clusters (Sect. 3.2). Also, we compare clustering performance of the deep clustering method with other popular clustering algorithms (Sect. 3.3).

3.1 Data and experimental settings

The Korean household finances and living conditions survey data were used in this study. This survey is conducted annually by the National Statistical Office of Korea, the Bank of Korea, and the Financial Supervisory Service of Korea to provide a solid ground for policymakers to account for households' financial soundness in terms of their level of income, assets, liabilities, and expenditures. Since the survey instrument was revised in 2017, we used data from 2017. The main analysis was done using survey data from 2017 to 2020. The total number of respondent households during that period was 54,920, and the number of unique households excluding multiple participation in different years was 26,907. In addition, the 2021 survey data of 18,187 households was used for out-of-sample analysis in Sect. 4.4. Note that the annual survey is conducted around every March. Hence, for example, the survey in 2020 is mostly based on households' financial activities in 2019. This means that our main analysis in Sects. 4.1–4.3 was done prior to COVID-19, and the out-of-sample analysis in Sect. 4.4 would show the changes after COVID-19.

For clustering purposes, we chose six asset-related variables, 12 debt-related variables, and seven expenditure-related variables for household balance sheets. The asset variables include deposit savings, other savings, long-term rental deposits, residential housing, non-residential real estate, other real assets. The debt variables include:

- *Mortgage loans*: Residential housing, nonresidential real estate, long-term rental deposit, living expenses, business, refinance
- *Credit loans*: Residential housing, nonresidential real estate, long-term rental deposit, living expenses, business, refinance

Expenditure variables include foodstuffs, housing, education, medical expenses, transportation, communication, other consumption expenditures. Other real assets include automobiles and valuables, and other consumption expenditures include spending on cultural life, clothing, alcohol, and tobacco. All variables are winsorized for the upper and lower 1% to handle extremely skewed distributions. In addition, they are divided by the total consumption expenditure to mitigate scale differences between households.

For demographic analysis, householder information (age, gender, education level, and employment status), number of household members, residential type, and location were used.

The specifications of the models are as follows: Both the encoder and decoder of the AE are fully connected multi-layer perceptrons (MLPs) with three hidden layers. All layers have rectified linear unit (ReLU) activation. The encoder MLP dimensions are d-100–100-200-k, where d is the dimensionality of the clustering variables and k is the number of clusters. That is, it receives a d-dimensional input, which goes through three hidden layers with 100, 100, and 200 neurons, respectively, and outputs a k-dimensional output. The decoder has an exactly opposite structure. Then, they are optimized using the Adam optimizer (Kingma & Ba, 2014). In Appendix A, we provide more detailed parameter settings and check the robustness of model outputs with respect to parameter choices. We confirm that our analysis would not be affected by small changes in parameters.

3.2 Number of clusters

We varied the number of clusters k from 4 to 12 to see how households are clustered as the number of clusters increases, and to determine the appropriate number of clusters for a more detailed analysis. Figure 3 shows the optimal clusters of household balance sheets obtained with different k, which is a hyperparameter that we should set before running the model. That is, circles with black color (label 4) represent optimal clusters when we set $k = 4$. Similarly, circles with light grey color (label 12) represent optimal clusters when we set $k = 12$. The location of a circle represents the median of total assets and total debt of households within each cluster, and the size of a circle indicates the average of the total expenditure of households within each cluster. Due to large scale differences in the total asset values of households, the asset axis is represented on a log-scale. The unit of all variables is KRW 10,000 ($\approx$ USD 10).

It can be seen from Fig. 3 that clusters are created along similar increasing curves of debt with respect to log(asset). In addition, there are a couple of clusters with very small total expenditures, while other clusters tend to have similar total spending. Hence, we would expect that there are more dimensions to household heterogeneity than total assets, total debt, and total expenditure. That is, we should investigate more detailed compositions of assets, debt, and expenditure to further understand household heterogeneity.

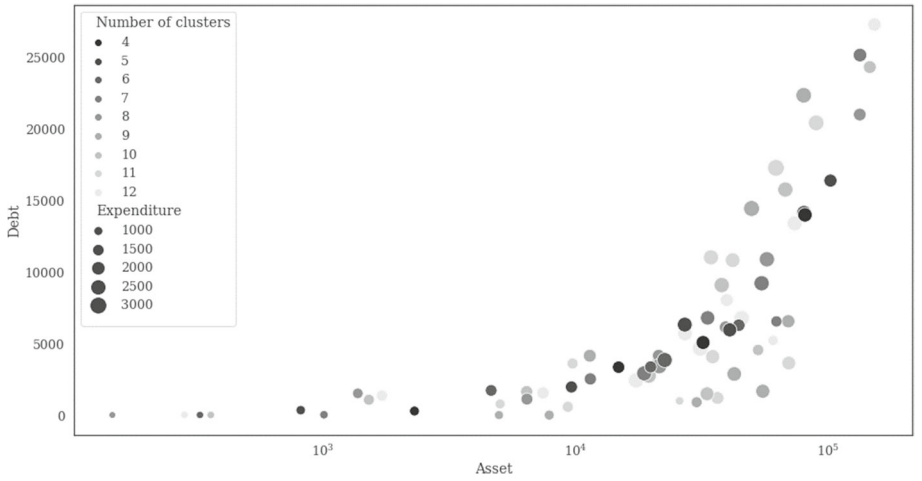

Fig. 3 Optimal household clusters with different number of clusters

Next, we determined the most appropriate k (number of clusters) for further analysis. There are households that appear in multiple years of the survey (17,887 out of 26,907). If they are assigned to different clusters in different years, it would result from either a significant change in the household balance sheet or unstable clustering. Thus, we keep track of these households and calculate the average of absolute changes in asset, debt, and expenditure variables. If the changes in the variables are small, it would mean that clustering is unstable. On the other hand, if the changes in the variables are large, it would imply that a household's cluster would change mostly when they had a significant change in their financial status, and thus, clustering would be stable. While the asset, debt, and expenditure variables are all used together for clustering, we calculated the changes in variables separately so that we may see more detailed aspects of the clustering results.

Table 1 shows the average absolute changes in assets, debt, expenditure variables in cluster

Table 1 Variable deviations and total count of cluster label changes

Experiments (k)	Average absolute difference of variables			Total count
	Asset	Debt	Expenditure	
4	0.261	0.391	0.071	7,473
5	0.235	0.308	0.069	8,587
6	0.233	0.335	0.069	9,554
7	0.239	0.333	0.070	12,202
8	**0.242**	**0.334**	**0.071**	**12,772**
9	0.226	0.347	0.067	14,458
10	0.230	0.313	0.070	15,767
11	0.222	0.316	0.067	16,212
12	0.231	0.308	0.070	16,548

changes, and total count of cluster changes. The average absolute differences indicate that cluster changes are caused by significant changes in debt and asset variables, while the effect of expenditure variables is relatively small. In terms of cluster numbers, note that the average absolute change of variables naturally decreases as the number of clusters increases because there are more clusters. For a similar reason, the total count of cluster changes tends to increase as the number of clusters increases. In this regard, the case of $k = 8$ (represented in bold) is particularly interesting because all variable changes are larger than in the case of $k = 7$ while the increment of total count is marginal compared to $k = 7$. That is, we would achieve relatively robust clusters when $k = 8$, thus, we fixed $k = 8$ for further analyses.

3.3 Model comparisons

Although we explained the reasons why we use a deep clustering method in Sect. 2, they should be backed up by performance comparisons. We compare our method (deep clustering via N2D) with four popular clustering methods, k-means, DBSCAN, hierarchical clustering (Ward's method), and hierarchical DBSCAN. k-means clustering would be the most well-known clustering algorithm that tries to separate data samples into k groups by choosing centroids that minimize the within-cluster variances. DBSCAN (Ester et al., 1996) is the acronym of density-based spatial clustering of applications with noise, which sums up its characteristics. It gathers points that are close to each other, while leaving out outliers. Hierarchical clustering methods aim to find clusters by building a hierarchy of clusters. There are various approaches depending on the linkage criterion that determines the dissimilarity between clusters. We use Ward's method, which can be seen as the hierarchical version of the k-means method. Lastly, the hierarchical DBSCAN is a hierarchical version of DBSCAN proposed by Schubert et al. (2017).

Clustering is a typical unsupervised learning task, and thus, the performance evaluation of clustering algorithms is not as trivial as regression models and classification models. The two most popular metrics are the Silhouette index and Davies-Bouldin index. The Silhouette index, proposed by Rousseeuw (1987), measures how each data point is similar to its own cluster compared to other clusters. The Davies-Bouldin index (Davies & Bouldin, 1979) represents the average similarity between each cluster and its closest cluster. Hence, good clusters would have a high Silhouette index but a low Davies-Bouldin index.

Table 2 summarizes the clustering performances of different methods. For each method, the number of clusters k is chosen to maximize the Silhouette index and minimize the Davies-Bouldin index. It is clear that the deep clustering method shows the best performance compared to other popular clustering methods in terms of two indexes in our dataset.

Table 2 Clustering performance comparison

	k-means	DBSCAN	Hierarchical clustering	Hierarchical DBSCAN	Deep clustering
	($k = 10$)	($k = 13$)	($k = 7$)	($k = 7$)	(***k* = 8**)
Silhouette (↑)	0.317	0.065	0.292	0.154	**0.381**
Davies-Bouldin index (↓)	1.418	1.278	1.515	1.553	**0.816**

4 Analysis of household heterogeneity via deep clustering

In this section, we find representative clusters of household balance sheets via deep clustering and analyze them. The optimal clusters are analyzed in detail in terms of financial (Sect. 4.1) and demographic (Sect. 4.2) perspectives. The inter-cluster mobility is discussed in Sect. 4.3. Finally, we present an out-of-sample analysis in Sect. 4.4.

4.1 Household heterogeneity in balance sheets

As we have seen from Fig. 1, the relationship between asset allocation and wealth level is highly nonlinear, and dividing households in terms of wealth level was not helpful in simplifying the relationship. We present the same results for all five income quintiles, four age groups (under 40, 40 to 50, 50 to 60, above 60), and 20 income-age groups in Appendix B. While households are often classified in terms of their income or age, these results indicate that such groups do not do much to reduce within-group heterogeneity.

Figure 4 represents the average portfolio weights with respect to wealth level of different household clusters found by the deep clustering method. We can clearly see that the relationship has become much simpler. In particular, asset allocations seem almost constant within Clusters 1 to 4. This shows what deep learning can do in analyzing complex household finance data. Deep learning has been exceptional in capturing nonlinear dependencies within data. Hence, it was able to group households accounting for complex relationships, and thus, groups have much higher within-group homogeneity.

We now investigate the financial heterogeneity of households in more detail. Table 3 summarizes the financial variables of eight clusters with units of KRW 10,000 ($\approx$ USD 10).[4] Clusters are sorted with respect to the average total asset value in descending order. Hence, Cluster 1 was the wealthiest group and Cluster 8 was the poorest group. The numbers in parentheses are proportions of each variable within the asset, debt, and expenditure categories. Values with relatively large proportions compared to other clusters are highlighted in bold.

For assets shown in Panel A of Table 3, there is a clear tendency that the wealthy-half (Clusters 1, 2, 3, 4) hold more than 50% of their assets in real estate (residential and nonresidential), while non-wealthy-half (Clusters 5, 6, 7, 8) hold more than 50% of their assets in financial assets (deposit savings, other savings, long-term rental deposits). Among the wealthy-half, the wealthiest two (Clusters 1 and 2) have a significant amount of nonresidential real estate, but the other two (Clusters 3 and 4) do not. As for the non-wealthy-half, Cluster 5 has more than 60% of their assets in long-term rental deposits, whereas Clusters 6 and 7 are more concentrated in savings and other real assets. Cluster 8 seems to be the poorest group with a very small amount of assets. Overall, the major asset classes of different household groups are summarized in Fig. 5.

It is widely known that Korean household wealth is excessively concentrated in real estate compared to other developed countries (Fredriksen, 2012; Park, 2020). However, our analysis reveals that this statement is true only for the wealthy-half groups. This shows the importance of analyzing heterogeneous household groups, because aggregated values would be naturally biased towards wealthy groups that possess large amounts of assets.

A similar tendency can be found for the debt variables (Panel B of Table 3). More than 30% of loans in Clusters 1 and 2 are for nonresidential real estate, and more than 60% of loans in Clusters 3 and 4 are for residential housing. Approximately 70% of the loans for Cluster 5 are for long-term rental deposits, and more than 70% of loans in Clusters 7

[4] More detailed statistics of household balance sheets of different clusters are given in Appendix C.

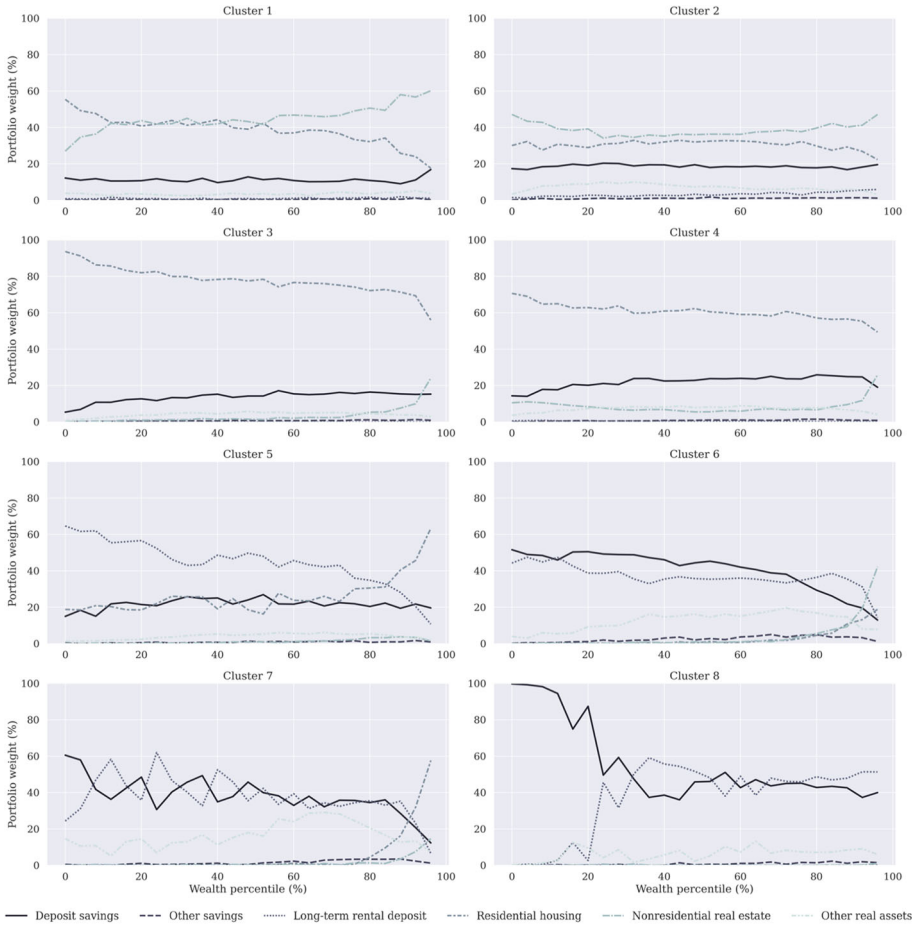

Fig. 4 Average portfolio weights of different household clusters

and 8 are for living expenses, business funds, and refinances. Hence, the purpose of loans changes from urgent financial liquidity to purchasing real estate as the household wealth level increases. In addition, more than 70% of the loans in Clusters 1 to 5 are mortgage loans, but the other clusters have more credit loans. Clusters 7 and 8 rarely have mortgage loans ($\leq$ 10%), probably due to a lack of underlying assets. Figure 6 summarizes the findings.

Panel C of Table 3 shows the expenditure variables for different household clusters. While the overall proportions are not as heterogeneous as in the asset and debt variables, a few interesting observations can be found. First, the poorest two clusters (7 and 8) spent a relatively large amount on housing ($\geq$ 20%) compared to the others. Second, Clusters 2 to 5 tended to invest more on education ($\geq$ 10%). Third, more than 10% of the expenditure of the poorest group (Cluster 8) is for medical purposes. Fourth, wealthy groups (Clusters 1 to 5) tend to spend slightly more (around 25%) for cultural life, clothing, alcohol, tobacco, etc. (categorized as 'others').

A rough decision tree is shown in Fig. 7 to summarize the multidimensional heterogeneity of household finance. We can see that asset and debt variables are more crucial for representing

Table 3 Average values (proportions) of asset, debt, expenditure variables of different household clusters

No	Deposit savings	Other savings	Long-term rental deposit	Residential housing	Nonresidential real estate	Other real assets
Panel A. Assets						
1	16,089.8 (12.1%)	662.4 (0.5%)	1343.1 (1.0%)	**42,702.6 (32.2%)**	**67,093.6 (50.6%)**	4673.1 (3.5%)
2	10,386.6 (18.4%)	801.0 (1.4%)	2470.8 (4.4%)	**16,426.5 (29.1%)**	**22,199.5 (39.3%)**	4167.7 (7.4%)
3	6507.1 (16.6%)	353.3 (0.9%)	1.1 (0.0%)	**30,408.0 (77.8%)**	227.3 (0.6%)	1589.6 (4.1%)
4	5189.1 (24.4%)	219.9 (1.0%)	82.1 (0.4%)	**12,662.5 (59.5%)**	1500.5 (7.1%)	1612.5 (7.6%)
5	**5822.6 (28.5%)**	327.1 (1.6%)	**12,501.0 (61.3%)**	1.1 (0.0%)	674.7 (3.3%)	1076.2 (5.3%)
6	**2735.1 (43.2%)**	**336.3 (5.3%)**	**2016.5 (31.8%)**	18.5 (0.3%)	95.4 (1.5%)	**1132.5 (17.9%)**
7	**469.7 (34.3%)**	**33.0 (2.4%)**	**474.8 (34.7%)**	31.3 (2.3.%)	18.5 (1.4%)	**339.4 (24.8%)**
8	**62.7 (42.5%)**	1.3(0.6%)	**78.2 (52.9%)**	0.0 (0.0%)	0.2 (0.1%)	5.2 (3.6%)

No	Residential housing	Nonresidential real estate	Long-term rental deposit	Living expense	Business funds	Refinance
Panel B-1. Debts (Mortgage loans)						
1	2185.7 (19.1%)	**4906.1** (42.9%)	87.4 (0.8%)	130.9 (1.1%)	**3208.7 (28.1%)**	123.9 (1.1%)
2	1699.0 (26.3%)	**1959.3** (30.3%)	228.2 (3.5%)	118.1 (1.8%)	**1382.6 (21.4%)**	108.4 (1.7%)
3	**4189.9 (81.8%)**	24.2 (0.5%)	27.5 (0.5%)	142.9 (2.8%)	259.5 (5.1%)	82.4 (1.6%)
4	**1712.2 (62.2%)**	90.3 (3.3%)	26.2 (1.0%)	136.3 (5.0%)	252.6 (9.2%)	75.3 (2.7%)
5	9.7 (0.3%)	75.9 (2.2%)	**2456.7** (70.7%)	56.8 (1.6%)	62.5 (1.8%)	16.9 (0.5%)
6	0.4 (0.1%)	3.7 (0.5%)	**146.4 (20.9%)**	60.6 (8.7%)	74.1 (10.6%)	14.9 (2.1%)
7	7.7 (1.3%)	0.5 (0.1%)	8.2 (1.3%)	15.5 (2.5%)	18.3 (3.0%)	5.1 (0.8%)
8	0.0 (0.0%)	0.0 (0.0%)	0.0 (0.0%)	0.0 (0.0%)	0.0 (0.0%)	0.0 (0.0%)
Panel B-2. Debts (Credit loans)						

Table 3 (continued)

No	Residential housing	Nonresidential real estate	Long-term rental deposit	Living expense	Business funds	Refinance
1	57.1 (0.5%)	232.3 (2.0%)	22.7 (0.2%)	100.5 (0.9%)	342.8 (3.0%)	36.1 (0.3%)
2	102.9 (1.6%)	213.4 (3.3%)	55.0 (0.9%)	161.6 (2.5%)	380.0 (5.9%)	50.9 (0.8%)
3	95.9 (1.9%)	15.5 (0.3%)	5.8 (0.1%)	135.4 (2.6%)	119.2 (2.3%)	25.4 (0.5%)
4	71.6 (2.5%)	32.9 (1.2%)	9.9 (0.4%)	187.6 (6.8%)	124.8 (4.5%)	31.4 (1.1%)
5	64.4 (1.9%)	125.4 (3.6%)	**336.1** (9.7%)	119.5 (3.4%)	136.5 (3.9%)	16.0 (0.5%)
6	6.0 (0.9%)	20.1 (2.9%)	**76.7 (11.0%)**	**141.7 (20.2%)**	**126.9 (18.1%)**	28.5 (4.1%)
7	1.6 (0.3%)	9.0 (1.5%)	**44.8 (7.3%)**	**188.5 (30.8%)**	**201.2 (32.9%)**	**111.8 (18.3%)**
8	0.0 (0.0%)	0.0 (0.0%)	0.0 (0.0%)	**0.6 (100.0%)**	0.0 (0.0%)	0.0 (0.0%)

No	Foodstuffs	Housing	Education	Medical	Transportation	Communication	Others
Panel C. Expenditures							
1	712.3 (31.4%)	292.0 (12.9%)	155.7 (6.9%)	189.3 (8.4%)	218.1 (9.6%)	125.0 (5.5%)	**572.7 (25.3%)**
2	856.1 (27.8%)	325.7 (10.5%)	**388.3 (12.5%)**	219.1 (7.0%)	327.3 (10.5%)	181.7 (5.8%)	**801.4 (25.8%)**
3	708.7 (31.4%)	257.9 (11.4%)	**230.9 (10.2%)**	164.2 (7.3%)	217.3 (9.6%)	142.5 (6.3%)	**537.5 (23.8%)**
4	885.2 (28.5%)	296.5 (9.5%)	**418.5 (13.5%)**	227.9 (7.3%)	323.7 (10.4%)	196.6 (6.3%)	**759.9 (24.4%)**
5	677.6 (31.2%)	260.5 (12.0%)	**234.3 (10.8%)**	117.5 (5.3%)	209.0 (9.6%)	145.5 (6.7%)	**528.3 (24.3%)**
6	604.3 (29.4%)	368.2 (17.9%)	165.8 (8.1%)	116.8 (5.7%)	207.5 (10.1%)	147.5 (7.2%)	447.2 (21.7%)
7	503.2 (29.5%)	**368.4 (21.6%)**	106.1 (6.2%)	107.6 (6.3%)	160.9 (9.4%)	125.7 (7.4%)	332.2 (19.5%)
8	339.7 (36.3%)	**210.5 (22.5%)**	18.4 (2.0%)	**110.0 (11.8%)**	54.1 (5.8%)	54.1 (5.8%)	148.5 (15.9%)

(Unit: KRW 10,000)

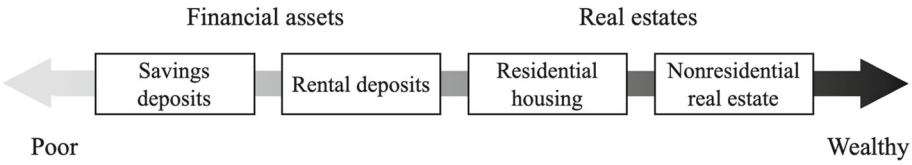

Fig. 5 Major asset class of households with different level of wealth

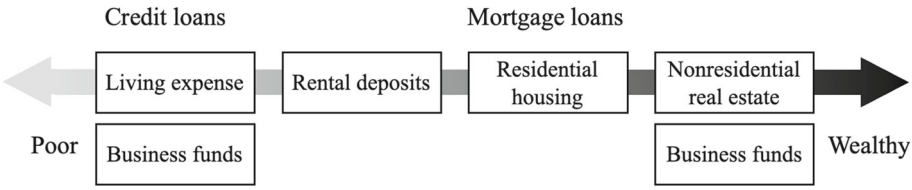

Fig. 6 Major loan types of households with different level of wealth‘

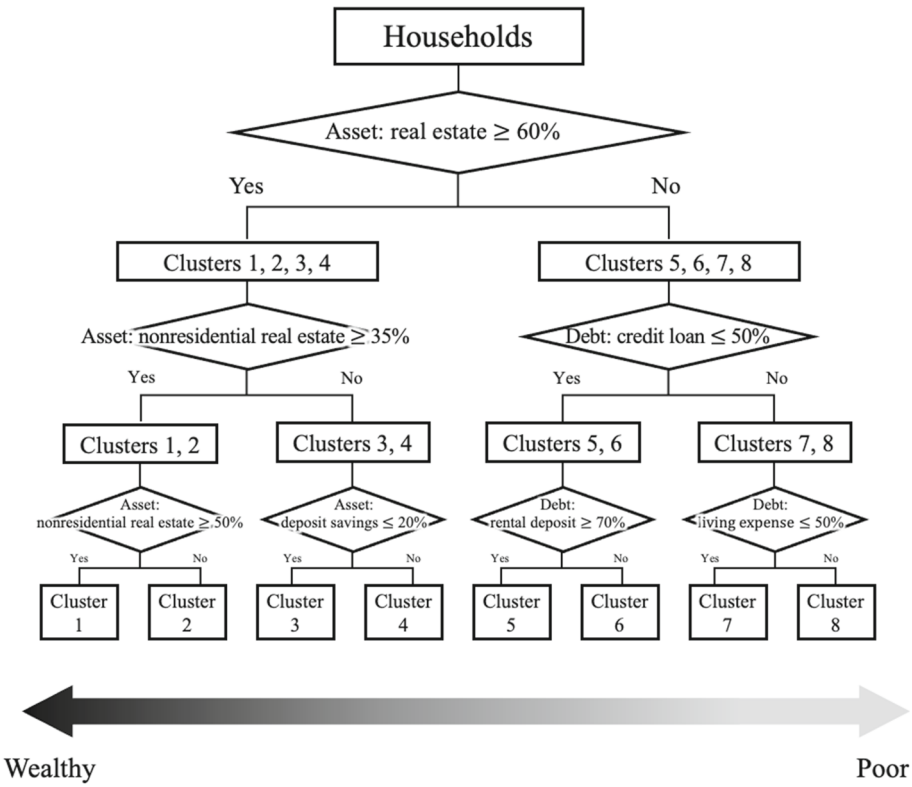

Fig. 7 Decision tree for household clusters

the heterogeneity of households than expenditure variables. For more detailed classifications, asset compositions (especially real estate) are important for wealthy groups, whereas the purpose and type of debt are important for non-wealthy groups.

4.1.1 Clustering quality and variable importance

Here we further check the quality of the clustering results and the importance of each variable by investigating how variables are distributed within and between groups. Recall that the objective of clustering is to find clusters with high within-cluster similarities and low between-cluster similarities. We believe that the Gini coefficient and its decomposition can be useful in this regard. The Gini coefficient is a popular measure of inequality in the distribution of income or wealth, and some researchers have decomposed the Gini coefficient to investigate the causes of disparity in income distributions with different populations and educational backgrounds (Deaton & Paxson, 1994, 1997). There are two popular approaches to decomposition: Pyatt (1976) and Shorrocks (1982). While the former directly compares the Gini coefficients of different groups, the latter linearly decomposes the Gini coefficient into within-group, between-group, and overlapping inequalities. We use the latter approach because it quantifies within-group and between-group inequalities that are exactly in line with the clustering objective.

Let us consider k groups (or clusters) and a variable Y. Y_I represents the variable within group i with mean μ_I and cumulative distribution $F_i(Y_i)$. Then, the overall population $Y_u = Y_1 \cup Y_2 \ldots \cup Y_k$ is the union of all groups with $F_u(Y_u) = \sum_i p_i F_i(Y_i)$, where p_I is the population share of group i, with mean μ_u. The Gini coefficient of the overall population is defined as.

$$G = \frac{2\mathrm{cov}(Y_u, F_u(Y_u))}{\mu_u},$$

and Mookherjee and Shorrocks (1982) decomposed it into

$$G = G_W + G_B + G_O.$$

Here, within-group inequality G_W is defined as $G_W = \sum_i p_i q_i G_i$, where q_i is the variable share of group i, $G_i = \frac{2\mathrm{cov}(Y_i, F_i(Y_i))}{\mu_i}$ is the Gini coefficient within group i. Between-group inequality G_B is defined as $G_B = \sum_i \sum_j \frac{p_i p_j |\mu_i - \mu_j|}{2\mu_u}$, and overlapping inequality G_O is the remainder.

We calculated within-group inequality (G_W), between-group inequality (G_B), and overlapping inequality (G_O) for all cluster variables, and the proportions of the three inequalities are shown in Fig. 8. Three important observations were made. First, we can see that all within-group inequalities are less than 20% and are mostly much less than between group inequalities. This indicates that the quality of clustering is good because all variables tend to have high within-group similarities and low between-group similarities. Second, there are some variables in which between-group inequality accounts for more than 60% of the Gini index. For example, long-term rental deposits, residential housing, nonresidential real estate, mortgage loans for nonresidential housing, long-term rental deposits, business funds, and credit loans for long-term rental deposits. All these variables were shown to be very important in interpreting the clustering results. Third, all expenditure variables exhibited more than 60% of the overlapping inequalities. That is, these variables do not contribute much to clustering, which is consistent with our previous discussion.

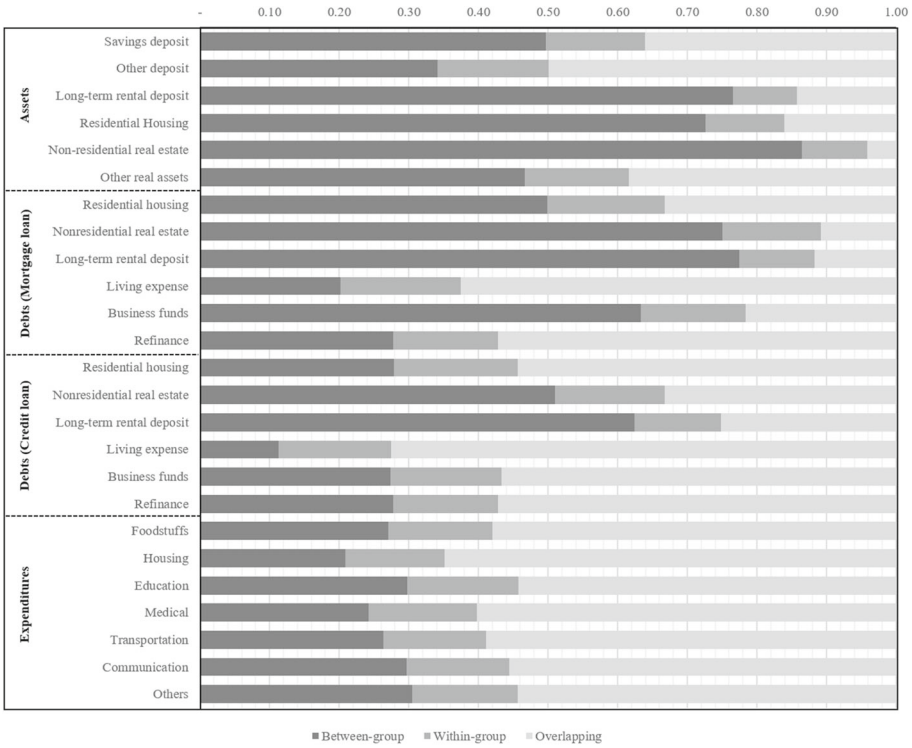

Fig. 8 Decomposition of Gini coefficients into between-group, within-group, and overlapping inequalities

Table 4 List of independent variables for logistic regression

Independent variable	Description
Area of residence	Living in Seoul metropolitan area or not
Gender of householder	Male or not
Number of family members	(Numbers are directly used for regression)
Education level of householder	Under middle school, high school, or higher education
Home ownership	None (includes monthly rental or free company housing), long-term rental, or homeowner
Age of householder	Under 39, 40 ~ 49, 50 ~ 59, or upper 60
Income level	Low-income (1st and 2nd income quintiles), mid-income (3rd income quintile), or high-income (4th and 5th income quintiles)
Employment status	Employed or not (includes freelancers or helping family business)

4.2 Sociodemographic characteristics of clusters

Although optimal clusters are found only with respect to a financial perspective, there is no doubt that household finance is closely related to sociodemographics, such as householder's age, education level, and so on. Therefore, we conducted logistic regressions for all clusters

Table 5 Logistic regression results of clusters with respect to socio-demographic variables

Variables	Cluster 1		Cluster 2		Cluster 3		Cluster 4	
	Coeff	Odds ratio	Coeff	Odds ratio	Coeff	Odds ratio	Coeff	Odds ratio
Constant	− 5.224***	0.005	− 3.972***	0.019	− 2.833***	0.059	− 3.025***	0.049
Metropolitan area	*0.642***	*1.900*	**− 0.646*** **	**0.524**	*0.622***	*1.863*	**− 0.977*** **	**0.376**
Gender (male)	*0.224***	*1.251*	*0.474***	*1.607*	− .109***	0.897	− 0.014	0.986
Number of members	**− 0.349*** **	**0.705**	0.062***	1.064	− 0.047***	0.954	*0.338***	*1.402*
Education (under middle school)								
High school	0.246***	1.279	− 0.064*	0.938	− 0.053	0.949	**− 0.353*** **	**0.702**
Higher education	*0.773***	*2.166*	0.129***	1.138	0.134***	1.143	**− 0.751*** **	**0.472**
Home ownership (none)								
Long-term rental	0.489***	1.630	0.597***	1.816	0.063	1.065	− 0.463***	0.629
Homeowner	1.486***	4.421	0.656***	1.927	*2.806***	*16.547*	*1.648***	*5.197*
Age (under 39)								
40 ~ 49	0.665***	1.945	0.596***	1.815	**− 0.304*** **	**0.738**	*0.385***	*1.470*
50 ~ 59	1.330***	3.780	1.000***	2.718	**− 0.584*** **	**0.558**	0.164***	1.178
Upper 60	*2.539***	*12.66*	*1.235***	*3.440*	**− 0.472*** **	**0.624**	− 0.485***	0.616
Income level (low-income)								
Mid-income	0.338***	1.403	0.356***	1.428	− 0.119***	0.888	− 0.031***	0.734
High-income	*0.812***	*2.252*	*0.799***	*2.224*	− 0.358***	0.699	− 0.257	0.773
Employment	0.012	1.012	*0.628***	*1.875*	**− 0.491*** **	**0.612**	0.193***	1.213
Number of households	5937		10,644		10,699		10,001	

Table 5 (continued)

Variables	Cluster 5		Cluster 6		Cluster 7		Cluster 8	
	Coeff	Odds ratio	Coeff	Odds ratio	Coeff	Odds ratio	Coeff	Odds ratio
Constant	− 1.402***	0.246	− 0.367***	0.693	− 0.088	0.916	− 0.107***	0.899
Metropolitan area	*0.794***	*2.212*	0.013	1.013	0.021	1.022	− 0.205**	0.815
Gender (male)	**− 0.411*** **	**0.663**	**− 0.225*** **	**0.799**	0.005	1.005	0.137**	1.147
Number of members	− 0.098***	0.906	0.004	1.004	− 0.068***	0.934	**− 0.525*** **	**0.592**
Education (under middle school)								
High school	− 0.050	0.951	0.204***	1.227	0.017	1.017	**− 0.599*** **	**0.549**
Higher education	*0.310***	*1.363*	− 0.188***	0.829	− 0.435***	0.647	**− 1.330*** **	**0.264**
Home ownership (None)								
Long-term rental	*2.197***	*8.995*	**− 0.979*** **	**0.376**	**− 2.421*** **	**0.089**	**− 2.414*** **	**0.089**
Homeowner	− 1.674***	0.187	**− 2.840*** **	**0.058**	**− 2.911*** **	**0.054**	**− 2.758*** **	**0.063**
Age (under 39)								
40 ~ 49	**− 0.578*** **	**0.561**	**− 0.170*** **	**0.843**	**− 0.177*** **	**0.838**	− 0.139	0.870
50 ~ 59	**− 0.850*** **	**0.427**	**− 0.368*** **	**0.692**	**− 0.251*** **	**0.778**	− 0.019	0.981
Upper 60	**− 0.957*** **	**0.384**	**− 0.823*** **	**0.439**	**− 0.810*** **	**0.445**	− 0.168	0.845
Income level (low-income)								
Mid-income	− 0.043	0.958	− 0.326***	0.722	**− 0.855*** **	**0.425**	**− 1.753*** **	**0.173**
High-income	− 0.331***	0.718	− 1.018***	0.361	**− 2.040*** **	**0.130**	**− 2.299*** **	**0.100**
Employment	− 0.031	0.970	*0.328***	*1.388*	**− 0.262*** **	**0.769**	**− 1.091*** **	**0.336**
Number of households	5614		6204		4223		1598	

*$p < .05$, **$p < .01$, ***$p < .001$

to investigate their sociodemographic characteristics. Consider a logistic regression for a cluster. The dependent variable y_i is defined to represent whether a household is in a cluster. The independent variables are presented in Table 4. (Detailed statistics with the percentage see Appendix A.1.)

Table 5 summarizes the results of logistic regressions. Regression coefficients with statistical significance and corresponding odd ratios are shown. Notable variables are highlighted with shadows: positive (italic) and negative (bold) relationships. We can see that most variables are statistically significant, while having both positive and negative values. It shows a strong relationship between the multidimensional heterogeneity of household finance and sociodemographics.

Clusters 1 and 2, the wealthiest two groups, were shown to consist of older households compared to others. They both tend to have a highly educated male householder, living in their own houses, and have a high income. While Cluster 2 households live outside the Seoul metropolitan area and are employed, Cluster 1 households live in or near Seoul and have a small number of family members with mixed employment status. Cluster 2 was also more likely to have more family members.

Cluster 3 is quite unique in that it is one of the wealthiest groups with their own houses in metropolitan areas, but its households are likely to be unemployed (including freelance or helping family business) and have low income. They can also be characterized as highly educated young households. Perhaps this peculiar cluster represents young households who inherited houses early.

Clusters 4 and 5 can be regarded as two middle-class groups. Cluster 4 can be characterized as living outside metropolitan areas, large families, homeowners, and low education, while Cluster 5 can be characterized as living in metropolitan areas, small families, long-term rental housing, high education, and high income. These reflect typical rural–urban differences in family size (Key, 1961), income (Lipton, 1977), education (van Maarseveen, 2020), and housing affordability (Lee & Jun, 2018).

Clusters 6 and 7 both consist of poor households who are relatively young, under temporary housing (mostly monthly rent), with no higher education. However, the former is likely to be employed, whereas the latter is not.

Cluster 8 clearly represents the most vulnerable households with very small families (high probability of being alone), low education, low income, low education, unemployed, and under temporary housing, regardless of their age. This cluster had the smallest number of constituents.

Let us summarize the findings with respect to variables.

Age	Old clusters are likely to be wealthy, which is natural in a sense that households would accumulate wealth during working ages. However, there were also two strong exceptions (Clusters 3 and 8)
Education	The three most wealthy clusters are highly educated while the three most poor clusters are poorly educated. For the two middle class groups, one in metropolitan area (Cluster 5) is highly educated and the other outside metropolitan area (Cluster 4) is poorly educated. Also, Cluster 3 is highly educated but has low income
Income	The two most wealthy clusters have high income, and the three most poor clusters have low income. However, three clusters in the middle exhibit mixed results (especially Cluster 3)

	1	2	3	4	5	6	7	8
1	0.44	0.18	0.13	0.07	0.06	0.06	0.04	0.02
2	0.10	0.48	0.12	0.13	0.05	0.06	0.04	0.01
3	0.08	0.12	0.47	0.16	0.06	0.06	0.04	0.01
4	0.05	0.15	0.15	0.47	0.04	0.07	0.05	0.02
5	0.07	0.11	0.12	0.08	0.43	0.12	0.05	0.02
6	0.06	0.10	0.11	0.10	0.10	0.42	0.10	0.01
7	0.06	0.10	0.10	0.09	0.06	0.17	0.36	0.06
8	0.06	0.09	0.10	0.09	0.07	0.09	0.15	0.36

Fig. 9 Transition matrix between household clusters

Number of family members	While there is no clear linear relationship between family size and wealth, it is interesting to note that the wealthiest and the poorest clusters are highly likely to consist of small families
Area of residence	No overall trend is found, but typical rural–urban differences can be seen between the two middle class groups (Clusters 4 and 5)

Previous studies have focused on finding a linear relationship between two variables. For example, researchers have reported the existence of a linear relationship between income and wealth (Lee et al., 2020), between education and wealth (Brückner & Gradstein, 2013; Boshara et al., 2015), and the absence of a linear relationship between income and wealth (Mueller, Buchholz, & Blossfeld, 2011). However, our results show that even if there is an overall trend between two variables, there is always a strong exception, making the relationship non-linear. Hence, considering multiple variables is crucial for understanding the complex relationship between financial and sociodemographic variables.

4.3 Mobility between clusters

We analyze the mobility between clusters by tracking the cluster movements of households who participated in the survey multiple times. From 2017 to 2020, clusters of 12,272 households out of 52,920 total respondent households changed. Figure 9 shows the transition matrix of the clusters. The number in cell (i, j) represents the probability of a household moving from cluster i to cluster j in the next survey.

Some block-diagonal shapes can be observed. Two large blocks can be seen within Clusters 1, 2, 3, 4 and within Clusters 5, 6, 7, 8. That is, not many households move from the wealthy groups to the non-wealthy groups and vice versa, which indicates that there are two separate classes that are not reachable to each other in a few years of term. It is interesting to note that Clusters 1, 2, 3, 4 mostly own their houses and Clusters 5, 6, 7, 8 do not.

In addition, there are small blocks between most adjacent clusters (e.g., between clusters 1–2, 3–4, 5–6, 6–7, 7–8). However, we can find another weak link between Clusters 2 and 3. Recall that the key difference between the two clusters was that Cluster 2 had a substantial amount of nonresidential real estate, but Cluster 3 had almost none. Therefore, real estate is not only a crucial factor for classifying households, but also a huge hurdle for households who wish to climb up the class ladder.

4.4 Out-of-sample analysis after COVID-19

Lastly, we show the out-of-sample results using the survey data in 2021, which is mostly based on financial activities of households in 2020. Hence, it will allow us to see the changes after COVID-19 pandemic.

Figure 10 represents the variable importance weights of between-group inequalities of Gini coefficients of asset and debt (mortgage and credit loans) variables. We can see from the figure that after COVID-19, between-group inequalities are decreased in asset variables, but they are increased in debt variables. This means that the changes in debt after COVID-19 are quite different for different clusters, while changes in assets would not. Hence, we can see that the impact of COVID-19 was quite asymmetric for household debt, but it was relatively even for household assets. This makes sense because COVID-19 caused immediate damage to the income of households who have their own business (e.g., restaurants or coffee shops), and many of them had to obtain additional loans.

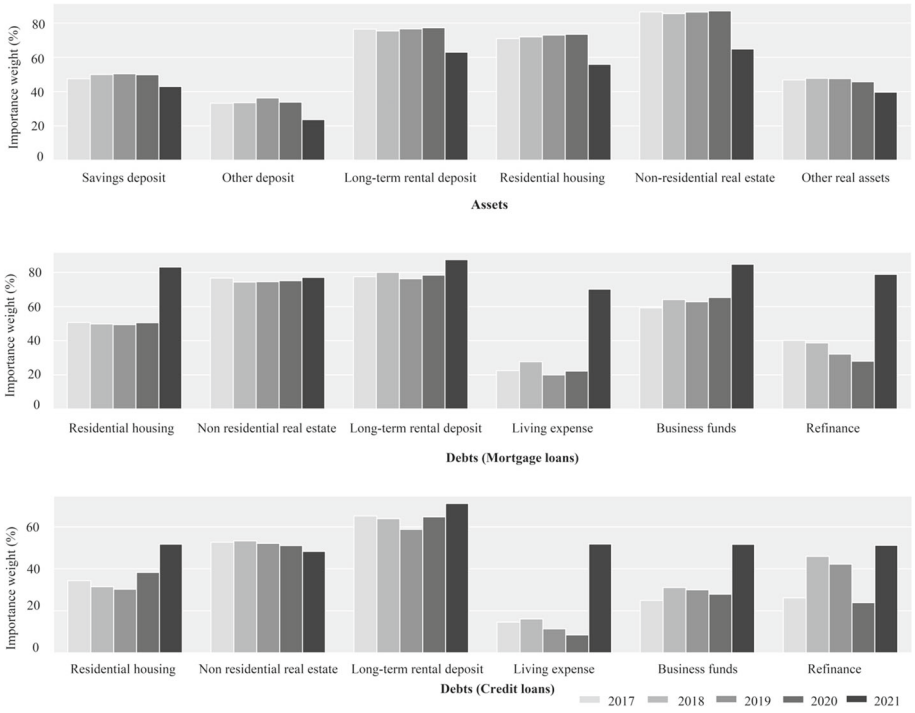

Fig. 10 Variable importance weights of between-group inequalities of Gini coefficients in different years

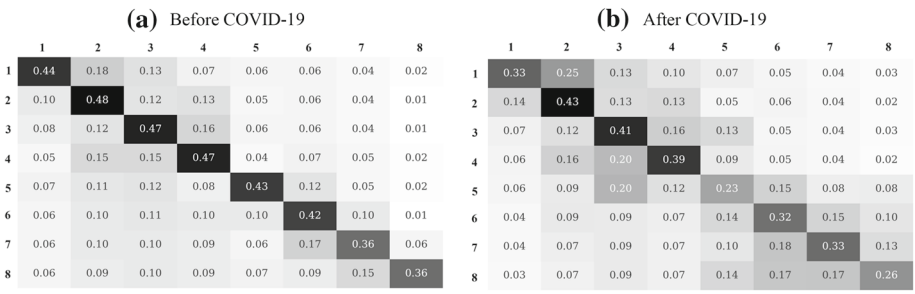

Fig. 11 Transition matrix between household clusters before (left) and after (right) COVID-19

Next, we investigate the change in mobility between clusters. Figure 11 compares the transition matrix before and after COVID-19. It is clear that the mobility is increased after COVID-19, because every diagonal term became smaller (i.e., probabilities of staying in the same cluster are reduced).

$$\frac{\text{Average probability of moving into a poorer cluster}}{\text{Average probability of moving into awealthier cluster}}$$

However, if we look into the above ratio[5] for the transition matrix, there is a significant difference between the wealthy half (Clusters 1,2,3,4) and the non-wealthy half (Clusters 5,6,7,8). Before COVID-19, the average of the above ratio for the transition matrix for the wealthy half and the non-wealthy half was 0.621 and 0.653, respectively. After COVID-19, however, they become 0.639 and 1.151. While the direction of cluster mobility for the wealthy half was not affected by COVID-19, it is clear that the probability of the non-wealthy half going into poorer clusters became much higher. Hence, we can see that COVID-19 had a much greater adverse impact for the non-wealthy half than the wealthy half.

5 Conclusion

This study has shown how advanced clustering techniques, especially that involve deep learning models, can be useful for understanding the complex heterogeneity of household finance. By utilizing a deep learning-based clustering N2D framework proposed by McConville et al. (2021), we were able to efficiently handle high-dimensional data to find representative clusters. More specifically, we could capture and decompose the nonlinear relationships in data through deep clustering, whereas conventional age or income groups could not.

The key implication of this study is that various variables should be considered together to analyze household heterogeneity. For example, real estate ownership was shown to be critical for the broad classification of wealthy and non-wealthy Korean households. Within the wealthy group, nonresidential real estate was shown to be the next key factor, while credit loans were found to be important explanatory variables for further classifications within the non-wealthy group. We used the Gini coefficients and their decompositions to further verify

[5] For the wealthy half (Clusters 1,2,3,4) before COVID-19, the numerator would be the average of the values on the right side of the first four diagonal values (0.18 + 0.13 + 0.07 + … + 0.04 + 0.07 + 0.05 + 0.02) / 22 = 0.0673. On the other hand, the denominator would be the average of the values on the left side of the first four diagonal values (0.10 + 0.08 + 0.12 + 0.05 + 0.15 + 0.15) / 6 = 0.1083. Hence, the ratio becomes 0.0673 / 0.108 = 0.621. The other ratios can be calculated similarly.

the quality of clustering and the relative importance of the variables. In addition, the multidimensional heterogeneity of households was shown to be closely related to sociodemographic variables, and the relationships were non-linear.

Since this study was conducted based on Korean household data, detailed findings should be interpreted carefully and might not be directly applicable to households in different countries. Hopefully, however, our study will encourage other researchers to search for more multidimensional aspects of household heterogeneity. Such findings are crucial for developing more accurate macroeconomic models with heterogeneous agents and deriving appropriate economic policies.

Acknowledgements This work was supported by the National Research Foundation of Korea (NRF) grant funded by the Korea government (MSIT) (No. NRF-2019R1C1C1010456). Fabozzi was funded by EDHEC Business School for the 2020-2021 academic year.

Appendix A: Hyperparameters for deep clustering

For autoencoder, we used a three-layer fully connected networks with rectified linear units (ReLU). While there are many different network architectures and activation functions, we have chosen one of the simplest forms to mitigate the architecture specific results. Note that ReLU is known to be more appropriate for sparse data compared to the sigmoid function (Glorot et al., 2011), and households' debt data are very sparse since there are many households who do not have any or some type of loan. In addition, we set the dropout rate as 0.05 for all layers for the robustness of the model.

Table 6 shows the range of hyperparameters we used to train deep clustering algorithm (autoencoder and UMAP). To find the optimal parameters, we used a random search approach (Bergstra & Bengio, 2012) by randomly sampling 200 models within the range. Note that the number of all combination is $4 \times 4 \times 4 \times 3 \times 2 = 384$, and thus, the random search covers more than 50%.

We have chosen the best model configuration among 200 randomly sampled model settings with respect to the Silhouette index and Davis-Bouldin index. Here, we show that our results are not restricted to this particular choice. In Fig. 12, we compare the box plot of Euclidean distance from the cluster centers of the best model for top 20 model configurations and the whole 200 random samples. To be more specific, we ordered clusters in terms of their average wealth for each model setting. Then, for a model configuration, we would have clusters 1 to 8. Next, we calculated the distance between the cluster $\boldsymbol{i}$ in each model configuration and the cluster $\boldsymbol{i}$ in the best model configuration, and we took the summation for all $\boldsymbol{i}$. In the figure, it is clear that the top 20 models have cluster centers that are very much close to the cluster centers from the best model. Hence, it means that the results shown in Sect. 4 would

Table 6 Hyperparameter search range

Hyperparameter	Range
Batch size	[16, 24, 32, 64]
Learning rate	[0.0001, 0.001, 0.001, 0.01]
Epochs	[20, 50, 75, 100]
# of nodes in each layer	[10–1000, 10–1000, 10–1000]
α, β(UMAP)	[0.9 ~ 1, 0.5–1.0]

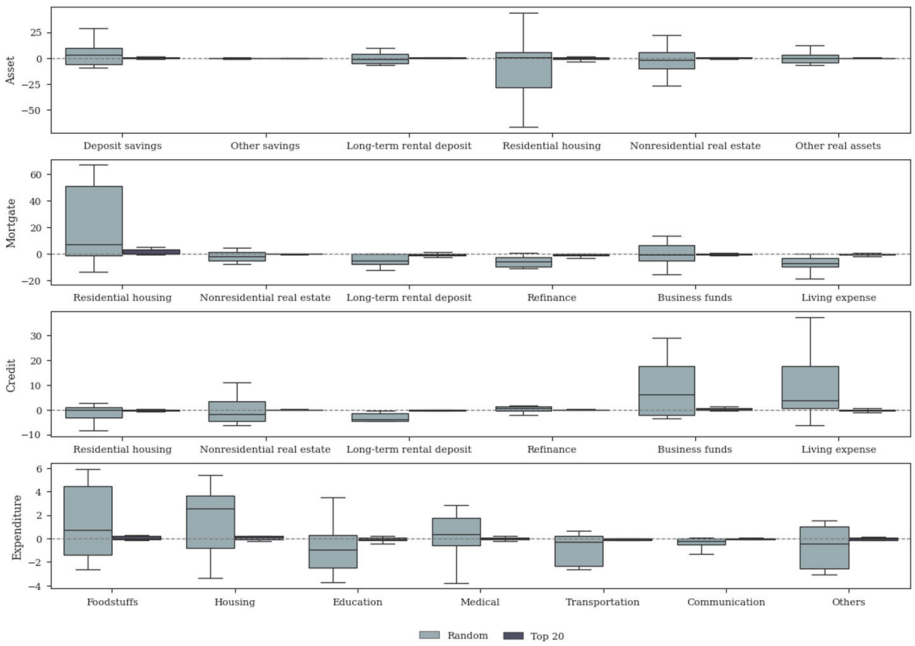

Fig. 12 Euclidian distance between the models

not change much even if we choose another model configuration within the top 20 model configurations with respect to the Silhouette index and Davies-Bouldin index.

Appendix B. Average portfolio weights of different income and age groups

See Figs. 13, 14, and 15.

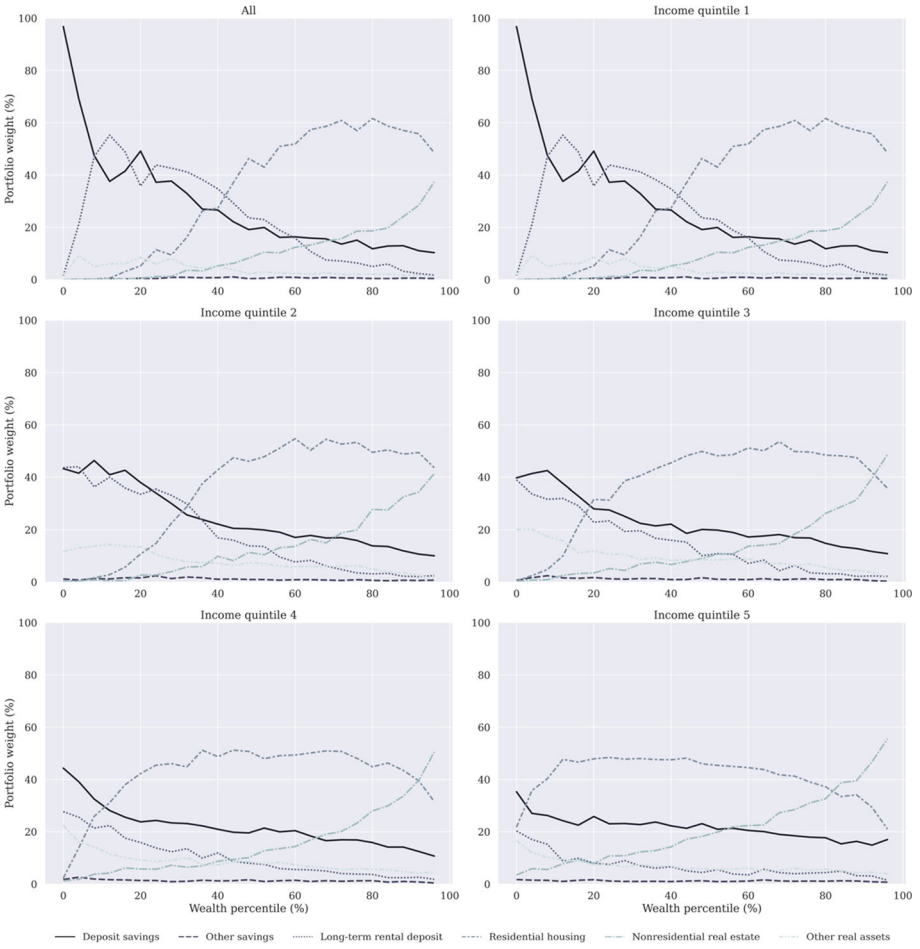

Fig. 13 Average portfolio weights of different income quintiles

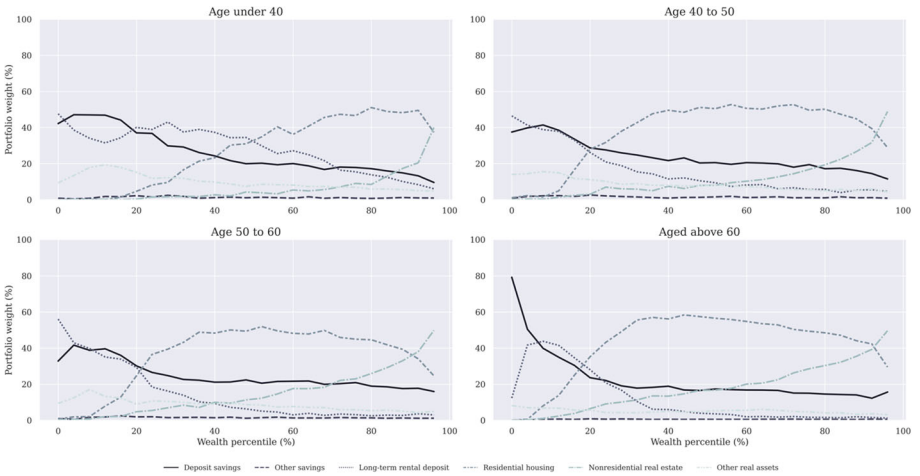

Fig. 14 Average portfolio weights of different age groups

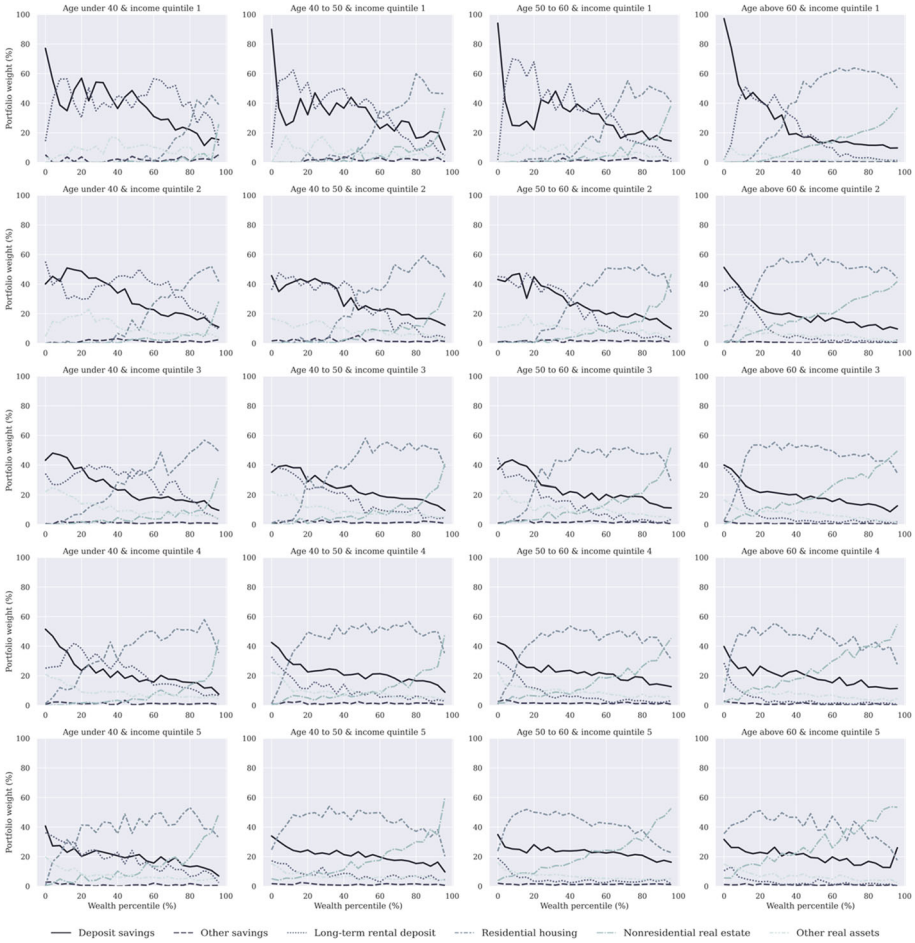

Fig. 15 Average portfolio weights of different income and age groups

Appendix C. Summary statistics of household balance sheet of clusters

See Table 7.

Table 7 Summary statistics of household balance sheet of clusters

Panel A. Assets

No	Deposit savings		Other savings		Long-term rental deposit		Residential housing		Nonresidential real estate		Other real assets	
	Mean (Std dev)	Median	Mean (Std dev)	Median	Mean (Std dev)	Median	Mean (Std dev)	Median	Mean (Std dev)	Median	Mean (Std dev)	Median
1	0.105 (0.128)	0.061	0.003 (0.019)	0.000	0.007 (0.039)	0.000	0.390 (0.303)	0.330	0.461 (0.294)	0.491	0.028 (0.068)	0.007
2	0.178 (0.159)	0.132	0.012 (0.047)	0.000	0.032 (0.091)	0.000	0.304 (0.226)	0.313	0.382 (0.242)	0.373	0.080 (0.137)	0.030
3	0.143 (0.139)	0.106	0.006 (0.029)	0.000	0.000 (0.010)	0.000	0.813 (0.157)	0.845	0.004 (0.020)	0.000	0.036 (0.056)	0.014
4	0.229 (0.157)	0.213	0.008 (0.032)	0.000	0.004 (0.029)	0.000	0.613 (0.246)	0.650	0.074 (0.175)	0.000	0.072 (0.087)	0.0447
5	0.254 (0.249)	0.173	0.010 (0.050)	0.000	0.654 (0.271)	0.712	0.000 (0.002)	0.000	0.015 (0.069)	0.000	0.043 (0.063)	0.017
6	0.467 (0.312)	0.441	0.002 (0.103)	0.000	0.359 (0.316)	0.297	0.001 (0.019)	0.000	0.005 (0.039)	0.000	0.130 (0.182)	0.474
7	0.418 (0.348)	0.327	0.011 (0.067)	0.000	0.389 (0.355)	0.322	0.004 (0.054)	0.000	0.003 (0.045)	0.000	0.174 (0.262)	0.000

Table 7 (continued)

Panel A. Assets

No	Deposit savings		Other savings		Long-term rental deposit		Residential housing		Nonresidential real estate		Other real assets	
	Mean (Std dev)	Median	Mean (Std dev)	Median	Mean (Std dev)	Median	Mean (Std dev)	Median	Mean (Std dev)	Median	Mean (Std dev)	Median
8	0.683 (0.408)	1.000	0.003 (0.042)	0.000	0.273 (0.401)	0.000	0.000 (0.021)	0.000	0.001 (0.029)	0.000	0.037 (0.147)	0.000

No	Residential housing		Nonresidential real estate		Long-term rental deposit		Living expense		Business funds		Refinance	
	Mean (Std dev)	Median	Mean (Std dev)	Median	Mean (Std dev)	Median	Mean (Std dev)	Median	Mean (Std dev)	Median	Mean (Std dev)	Median
Panel B-1. Debts (Mortgage loans)												
1	0.295 (0.432)	0.000	0.328 (0.446)	0.000	0.017 (0.125)	0.000	0.042 (0.192)	0.000	0.229 (0.406)	0.000	0.021 (0.134)	0.000
2	0.341 (0.450)	0.000	0.270 (0.421)	0.000	0.036 (0.178)	0.000	0.052 (0.211)	0.000	0.228 (0.407)	0.000	0.021 (0.139)	0.000
3	0.814 (0.375)	1.000	0.004 (0.060)	0.000	0.006 (0.078)	0.000	0.060 (0.230)	0.000	0.043 (0.195)	0.000	0.021 (0.136)	0.000
4	0.669 (0.456)	1.000	0.032 (0.168)	0.000	0.011 (0.099)	0.000	0.098 (0.287)	0.000	0.100 (0.293)	0.000	0.030 (0.168)	0.000
5	0.003 (0.059)	0.000	0.012 (0.103)	0.000	0.868 (0.328)	0.000	0.054 (0.220)	0.000	0.027 (0.157)	0.000	0.008 (0.088)	0.000

Table 7 (continued)

No	Residential housing		Nonresidential real estate		Long-term rental deposit		Living expense		Business funds		Refinance	
	Mean (Std dev)	Median	Mean (Std dev)	Median	Mean (Std dev)	Median	Mean (Std dev)	Median	Mean (Std dev)	Median	Mean (Std dev)	Median
6	0.002 (0.044)	0.000	0.007 (0.083)	0.000	0.439 (0.478)	0.000	0.288 (0.442)	0.000	0.133 (0.332)	0.000	0.041 (0.195)	0.000
7	0.024 (0.153)	0.000	0.004 (0.069)	0.000	0.186 (0.388)	0.000	0.428 (0.488)	0.000	0.175 (0.379)	0.000	0.038 (0.187)	0.000
8	0.000 (0.000)	0.000	0.000 (0.000)	0.000	0.000 (0.000)	0.000	0.000 (0.000)	0.000	0.000 (0.000)	0.000	0.000 (0.000)	0.000
Panel B-2. Debts (credit loans)												
1	0.054 (0.225)	0.000	0.124 (0.324)	0.000	0.016 (0.122)	0.000	0.323 (0.462)	0.000	0.375 (0.479)	0.000	0.022 (0.146)	0.000
2	0.061 (0.236)	0.000	0.110 (0.305)	0.000	0.037 (0.185)	0.000	0.316 (0.454)	0.000	0.327 (0.462)	0.000	0.030 (0.165)	0.000
3	0.130 (0.329)	0.000	0.013 (0.113)	0.000	0.015 (0.121)	0.000	0.497 (0.491)	0.333	0.156 (0.356)	0.000	0.040 (0.191)	0.000
4	0.081 (0.267)	0.000	0.021 (0.141)	0.000	0.010 (0.099)	0.000	0.506 (0.489)	0.500	0.178 (0.377)	0.000	0.046 (0.203)	0.000
5	0.018 (0.133)	0.000	0.049 (0.211)	0.000	0.294 (0.446)	0.000	0.343 (0.465)	0.000	0.104 (0.301)	0.000	0.025 (0.148)	0.000
6	0.006 (0.080)	0.000	0.012 (0.108)	0.000	0.132 (0.330)	0.000	0.419 (0.478)	0.000	0.232 (0.413)	0.000	0.054 (0.218)	0.000
7	0.001 (0.003)	0.000	0.001 (0.036)	0.000	0.092 (0.281)	0.000	0.436 (0.480)	0.000	0.168 (0.366)	0.000	0.109 (0.301)	0.000

Table 7 (continued)

No	Residential housing		Nonresidential real estate		Long-term rental deposit		Living expense		Business funds		Refinance	
	Mean (Std dev)	Median	Mean (Std dev)	Median	Mean (Std dev)	Median	Mean (Std dev)	Median	Mean (Std dev)	Median	Mean (Std dev)	Median
8	0.000 (0.000)	0.000	0.000 (0.000)	0.000	0.000	0.000	0.430 (0.498)	0.152	0.000 (0.000)	0.000	0.000 (0.000)	0.000

Panel C. Expenditures

No	Foodstuffs		Housing		Education		Medical		Transportation		Communication		Others	
	Mean (Std dev)	Median	Mean (Std dev)	Median	Mean (Std dev)	Median	Mean (Std dev)	Median	Mean (Std dev)	Median	Mean (Std dev)	Median	Mean (Std dev)	Median
1	0.335 (0.131)	0.323	0.157 (0.090)	0.136	0.033 (0.090)	0.000	0.098 (0.103)	0.064	0.094 (0.068)	0.080	0.060 (0.036)	0.054	0.219 (0.124)	0.200
2	0.296 (0.115)	0.283	0.121 (0.082)	0.098	0.081 (0.126)	0.000	0.084 (0.105)	0.046	0.110 (0.070)	0.097	0.063 (0.033)	0.057	0.241 (0.121)	0.226
3	0.338 (0.125)	0.326	0.139 (0.079)	0.118	0.060 (0.111)	0.000	0.089 (0.104)	0.057	0.093 (0.065)	0.059	0.066 (0.036)	0.059	0.213 (0.118)	0.196
4	0.302 (0.116)	0.290	0.110 (0.079)	0.088	0.096 (0.127)	0.000	0.087 (0.120)	0.041	0.106 (0.066)	0.095	0.066 (0.033)	0.061	0.230 (0.119)	0.215
5	0.337 (0.127)	0.322	0.146 (0.101)	0.115	0.062 (0.111)	0.000	0.064 (0.083)	0.033	0.095 (0.066)	0.065	0.073 (0.040)	0.065	0.220 (0.125)	0.205
6	0.310 (0.119)	0.297	0.203 (0.131)	0.176	0.053 (0.099)	0.000	0.063 (0.091)	0.029	0.095 (0.069)	0.081	0.073 (0.040)	0.066	0.200 (0.118)	0.181
7	0.341 (0.126)	0.297	0.235 (0.131)	0.217	0.037 (0.086)	0.000	0.070 (0.104)	0.031	0.087 (0.068)	0.069	0.072 (0.042)	0.063	0.181 (0.112)	0.163
8	0.381 (0.141)	0.376	0.234 (0.128)	0.215	0.009 (0.047)	0.000	0.121 (0.141)	0.070	0.054 (0.048)	0.041	0.055 (0.040)	0.044	0.142 (0.103)	0.118

References

Ahmad, A., & Khan, S. S. (2019). Survey of state-of-the-art mixed data clustering algorithms. *IEEE Access, 7*, 31883–31902.

Ahn, S., Kaplan, G., Moll, B., Winberry, T., & Wolf, C. (2018). When inequality matters for macro and macro matters for inequality. *NBER Macroeconomics Annual, 32*(1), 1–75.

Alzubaidi, L., Zhang, J., Humaidi, A. J., Al-Dujaili, A., Duan, Y., Al-Shamma, O., et al. (2021). Review of deep learning: Concepts, CNN architectures, challenges, applications, future directions. *Journal of Big Data, 8*(1), 1.

Atkinson, A. B., Piketty, T., & Saez, E. (2011). Top incomes in the long run of history. *Journal of Economic Literature, 49*(1), 3–71.

Bengio, Y., Courville, A. C., & Vincent, P. (2012). Unsupervised feature learning and deep learning: A review and new perspectives. Technical Report arXiv:1206.5538, U. Montreal (2012). Available at http://arxiv.org/abs/1206.5538

Bengio, Y., Courville, A. C., & Vincent, P. (2013). Representation learning: A review and new perspectives. *IEEE Transactions on Pattern Analysis and Machine Intelligence, 35*(8), 1798–1828.

Bergstra, J., & Bengio, Y. (2012). Random search for hyper-parameter optimization. *Journal of Machine Learning Research, 13*(2), 281–305.

Berton, F., Mocetti, S., Presbitero, A. F., & Richiardi, M. (2018). Banks, firms, and jobs. *The Review of Financial Studies, 31*(6), 2113–2156.

Boshara R, Emmons, W. R., & Noeth, B. J. (2015). The demographics of wealth. Available at http://www.stlouisfed.org/household-financial-stability/the-demographics-of-wealth. *Federal Reserve Bank of St. Louis*

Bricker, J., Krimmel, J., & Ramcharan, R. (2021). Signaling status: The impact of relative income on household consumption and financial decisions. *Management Science, 67*(4), 1993–2009.

Brückner, M., & Gradstein, M. (2013). *Income and schooling*. (No. DP9365) CEPR discussion papers. Available at SSRN. Available at https://ssrn.com/abstract=2224290

Burges, C. J. (2010). *Dimension reduction: A guided tour*. Now Publishers Inc.

Calvet, L. E., Campbell, J. Y., Gomes, F., & Sodini, P. (2021). *The cross-section of household preferences. (No, w. 28788)*. National Bureau of Economic Research.

Campbell, J. Y. (2006). Household finance. *The Journal of Finance, 61*(4), 1553–1604.

Caron, M., Bojanowski, P., Joulin, A., & Douze, M. (2018). Deep clustering for unsupervised learning of visual features. In. *Lecture notes in computer science.* Proceedings of the European conference on computer vision (ECCV) (pp. 139–156)

Case, K. E., Quigley, J. M., & Shiller, R. J. (2005). Comparing wealth effects: The stock market versus the housing market. *The B.E. Journal of Macroeconomics*, *5*(1), 1–34.

Case, K. E., Quigley, J. M., & Shiller, R. J. (2011). *Wealth effects revisited 1978–2009*. *National Bureau of Economic Research* (No, w. 16848)

Constantinides, G. M., & Duffie, D. (1996). Asset pricing with heterogeneous consumers. *Journal of Political Economy, 104*(2), 219–240.

Das, S., Kuhnen, C. M., & Nagel, S. (2020). Socioeconomic status and macroeconomic expectations. *The Review of Financial Studies, 33*(1), 395–432.

Davies, D. L., & Bouldin, D. W. (1979). A cluster separation measure. *IEEE Transactions on Pattern Analysis and Machine Intelligence, 2*, 224–227.

Deaton, A., & Paxson, C. (1994). Intertemporal choice and inequality. *Journal of Political Economy, 102*(3), 437–467.

Deaton, A. S., & Paxson, C. H. (1997). The effects of economic and population growth on national saving and inequality. *Demography, 34*(1), 97–114.

Dizioli, A., & Pinheiro, R. (2021). Information and inequality in the time of a pandemic. *Journal of Economic Dynamics and Control, 130*, 104202.

Donoho, D. L., & Grimes, C. (2003). Hessian eigenmaps: Locally linear embedding techniques for high-dimensional data. *Proceedings of the National Academy of Sciences of the United States of America, 100*(10), 5591–5596.

Eichenbaum, M. S., Rebelo, S., & Trabandt, M. (2021). *Inequality in life and death. (No, w. 29063)*. National Bureau of Economic Research.

Ester, M., Kriegel, H. P., Sander, J., & Xu, X. (1996). A density-based algorithm for discovering clusters in large spatial databases with noise. In *Proceedings of the second international conference on knowledge discovery and data mining (KDD-96)*. AAAI Press. Pp. 226–231.

Fredriksen, K. B. (2012). *Less income inequality and more growth-are they compatible? Part 6. The distribution of wealth*

Ghasedi Dizaji, K., Herandi, A., Deng, C., Cai, W., & Huang, H. (2017). Deep clustering via joint convolutional autoencoder embedding and relative entropy minimization. In *Proceedings of the IEEE international conference on computer vision (ICCV)* (pp. 5736–5745)

Glorot, X., Bordes, A., & Bengio, Y. (2011). Deep sparse rectifier neural networks. In *Proceedings of the fourteenth international conference on artificial intelligence and statistics* (pp. 315–323). JMLR workshop and conference proceedings.

Goodfellow, I., Pouget-Abadie, J., Mirza, M., Xu, B., Warde-Farley, D., Ozair, S. et al. (2014). Generative adversarial nets. *Advances in Neural Information Processing Systems*, *27*

Guo, X., Gao, L., Liu, X., & Yin, J. (2017). Improved deep embedded clustering with local structure preservation. In *International joint conference on artificial intelligence (IJCAI)*, pp. 1753–1759

Heaton, J., & Lucas, D. (1997). Market frictions, savings behavior, and portfolio choice. *Macroeconomic Dynamics, 1*(1), 76–101.

Jappelli, T., & Pistaferri, L. (2014). Fiscal policy and MPC heterogeneity. *American Economic Journal: Macroeconomics, 6*(4), 107–136.

Kingma, D. P., & Ba, J. (2014). *Adam: A method for stochastic optimization. arXiv preprint* arXiv:1412.6980

Krueger, D., Mitman, K., & Perri, F. (2016). Macroeconomics and household heterogeneity. In Taylor, J.B. & Uhlig, H. (eds) *Handbook of macroeconomics* (Vol. 2, pp. 843–921)1 Edn., Elsevier

Krueger, D., & Perri, F. (2006). Does income inequality lead to consumption inequality? Evidence and theory. *Review of Economic Studies, 73*(1), 163–193.

Krusell, P., & Smith, A. A. (1997). Income and wealth heterogeneity, portfolio choice, and equilibrium asset returns. *Macroeconomic Dynamics, 1*(2), 387–422.

Lee, K.-Y., & Jun, H.-J. (2018). Determinants of housing affordability among renters and homeowners: Comparison between the capital and non-capital regions. *Journal of Korea Planning Association, 53*(4), 143–161.

Lee, S. K., Shin, H. J., & Kim, C. H. (2020). Inequality of the household income and wealth in Korea: Research outcome and agenda. *Economy and Society, 127*, 60–94.

Lucas, D. J. (1994). Asset pricing with undiversifiable income risk and short sales constraints. *Journal of Monetary Economics, 34*(3), 325–341.

Mankiw, N. G., & Zeldes, S. P. (1991). The consumption of stockholders and nonstockholders. *Journal of Financial Economics, 29*(1), 97–112.

McConville, R., Santos-Rodriguez, R., Piechocki, R. J., & Craddock, I. (2021). (Not too) deep clustering via clustering the local manifold of an autoencoded embedding. In 2020. N2d 25th *international conference on* pattern recognition *(ICPR)*, pp. 5145–5152. IEEE

McInnes, L., Healy, J., & Melville, J. (2018). *Umap: Uniform manifold approximation and projection for dimension reduction. arXiv preprint* arXiv:1802.03426

Mookherjee, D., & Shorrocks, A. (1982). A decomposition analysis of the trend in UK income inequality. *The Economic Journal, 92*(368), 886–902.

Mueller, N., Buchholz, S., & Blossfeld, H. P. (2011). *Wealth inequality in Europe and the delusive egalitarianism of Scandinavian countries*. University of Bamberg.

Mukherjee, S., Asnani, H., Lin, E., & Kannan, S. (2019). Clustergan: Latent space clustering in generative adversarial networks. In. *Proceedings of the AAAI conference on artificial intelligence.*, 33, 4610–4617 (Vol. 33, No. 01, pp. 4610–4617)

OECD, A. (2018). *A broken social elevator? How to promote social mobility. COPE Policy Brief*

OECD (2021). *Fertility rates (indicator)*. https://doi.org/10.1787/8272fb01-en

Park, C. G. (2020). Long-term trends in the Korean financial sector and Covid-19, *Korea Capital Market Institute (KCMI) Issue Report*, 20–22

Piketty, T. (2013). *Capital in the 21st Century*. President and Fellows, Harvard College.

Pyatt, G. (1976). On the interpretation and disaggregation of Gini coefficients. *The Economic Journal, 86*(342), 243–255.

Rousseeuw, P. J. (1987). Silhouettes: A graphical aid to the interpretation and validation of cluster analysis. *Journal of Computational and Applied Mathematics, 20*, 53–65.

Saxena, A., Prasad, M., Gupta, A., Bharill, N., Patel, O. P., Tiwari, A., et al. (2017). A review of clustering techniques and developments. *Neurocomputing, 267*, 664–681.

Schubert, E., Sander, J., Ester, M., Kriegel, H. P., & Xu, X. (2017). DBSCAN revisited, revisited: Why and how you should (still) use DBSCAN. *ACM Transactions on Database Systems (TODS), 42*(3), 1–21.

Shorrocks, A. F. (1982). Inequality decomposition by factor components. *Econometrica, 50*(1), 193–211.

Tenenbaum, J. B., De Silva, V., & Langford, J. C. (2000). A global geometric framework for nonlinear dimensionality reduction. *Science, 290*(5500), 2319–2323.

Van der Maaten, L., & Hinton, G. (2008). Visualizing data using t-SNE. *Journal of Machine Learning Research, 9*(11), 2579–2605.

World Bank, *World Development Indicators* (2021). GDP (current US$) [Data file]. Available at https://data.worldbank.org/indicator/NY.GDP.MKTP.CD

Xia, W., Zhang, Y., Yang, Y., Xue, J. H., Zhou, B., & Yang, M. H. (2021). *Gan inversion: A survey. arXiv preprint* arXiv:2101.05278

Xie, J., Girshick, R., & Farhadi, A. (2016). Unsupervised deep embedding for clustering analysis. In *International Conference on Machine Learning,* 478–487.

Zhang, Z., & Wang, J. (2007). MLLE: Modified locally linear embedding using multiple weights. In *Advances in Neural Information Processing Systems*, 1593–1600

Portfolio Optimization with Quantum Generative Adversarial Networks

MyeongSu Choi, *Ph.D Candidate, Hanyang University*
Hyoung-Goo Kang[*], *Associate Professor, Hanyang University*

Abstract

Time series forecasting is an important area of financial forecasting. With advances in machine learning and AI, the speed of information drives market efficiency. A robust financial model assumes an efficient market in which all currently available information is factored into prices, and future prices are determined by uncertainty. Today's portfolio theory is based on the Markowitz framework, which focuses on market uncertainty analysis rather than price prediction. The Markowitz framework makes strong assumptions about the probability distribution of future returns. To overcome this drawback, we propose a generative adversarial network method using a quantum computer (QuGAN) for portfolio optimization. Generative models in QuGAN learn the probability distribution of asset prices to match the probability distribution in the real market. After training the model, we construct an optimal portfolio that minimizes risk and maximizes profit observed under various simulations. This study compares the portfolio through the QuGAN methodology and the classic Markowitz portfolio.

Keywords: Portfolio Optimization; Quantum GAN; Quantum Portfolio; Quantum Finance; Quantum Machine Learning

[*] Corresponding author: Hanyang University Business School, 222 Wangsimni-ro, Seongdong-gu, Seoul, 04763, Korea. Tel: +82-2-2220-2883, email: hyoungkang@hanyang.ac.kr

1. Introduction

Financial markets play a significantly important role in the modern economy. The financial market is where systematic financial transactions are made between the source of funds and the demand for funds. A product called a financial asset or financial instrument is required for a financial transaction. The investment industry has undergone significant changes in recent years due to machine learning and AI (Jaeger et al., 2020). However, financial portfolio management today is mainly based on linear models and the Markowitz framework known as Modern Portfolio Theory (MPT) (Markowitz, 1959). Despite its importance, the MPT is criticized for making idealistic assumptions about financial markets. MPT is determined as an estimate of future returns and volatility for each asset and its correlation. However, market price forecasting remains one of the significant challenges in the time series literature due to its noisy character (Tsay, 2005).

Data in financial markets are volatile and change rapidly over time. Traders need to make decisions in real time amid quickly changing information. This real-time information creates an efficient market. Current trading prices reflect all information and future data available to market participants. When meaningful long-term predictions are made in efficient markets, these predictions are already reflected in the short-term markets traders are trading (Timmermann & Granger, 2004). In other words, future forecasts affect current prices, and future prices again become uncertain.

Developing financial transactions and institutions increases market efficiency while making market prices challenging to predict. Recently, as convolutional neural networks (CNN) are gradually developed, research in various directions has been proposed (Krizhevsky et al., 2017). Among them, research on generative models has been actively conducted, and Goodfellow et al. (2014) first proposed a Generative Adversarial Networks (GAN) model in which generators and discriminators compete with each other for learning. Afterward, the generative model using these outputs a clear result similar to the actual photo and can create a new sample similar to the learning data by itself through the distribution of the learning data, so it is widely used in young fields and shows excellent performance.

In addition, various studies are being conducted to apply quantum computers to machine learning. One of them is a GAN using a quantum computer. Quantum generative adversarial networks (QuGAN) use the interaction of generators and discriminators to map an approximate representation of the probability distribution underlying a given data sample onto a quantum channel (Assouel et al., 2022). The generator and discriminator are trained in alternating optimization steps. The generator aims to generate samples that the discriminator will classify as training data samples (i.e., samples drawn from the actual training distribution), and the discriminator attempts to discriminate the original training. The generator's data sample and the data sample (i.e., distinguishes between real and generated distributions). The final goal is for the quantum generator to learn a representation of the underlying probability distribution of the training data. Thus, a trained quantum generator can load quantum states

that are approximate models of the target distribution.

This study presents pioneering research on building optimized portfolios using QuGAN. Our models use historical price data to predict future price trends related to non-linear interactions between different assets. We propose a methodology for constructing an arbitrary portfolio utilizing the distribution of accurate market data learned through QuGAN training. We specify the best portfolio diversification that minimizes the observed risk and maximizes the expected return. The main contributions of this paper are as follows.

First, unlike existing work and practice, this paper automatically learns non-linear market behavior and non-linear dependencies between different financial assets by modeling market uncertainty conditioned on the most recent past and generating many realistic future trends from the current situation. Second, to solve the portfolio diversification problem, we propose a real-time series generation model called QuGAN and an optimization methodology using the QuGAN model. The probability distribution learned by QuGAN allows you to use different options to offset the risk on your return. Third, experiments on real data sets show that the proposed approach can realize the risk-return tradeoff and far outperforms conventional MPT.

The rest of the paper is structured as follows. After introducing MPT in Section 2, we briefly review related work in Section 3. We present the QuGAN methodology proposed in Section 4. This includes market uncertainty modeling, generative network architecture, and an optimization approach for portfolio diversification decisions. Section 5 presents some experimental results demonstrating the effectiveness of QuGAN on real-world financial assets and data. Finally, Section 6 concludes the thesis.

2. Portfolio optimization with Markowitz's framework

Modern Portfolio Theory (MPT) is a practical method for selecting investments to maximize overall return within an acceptable level of risk. This mathematical framework is used to construct an investment portfolio that maximizes the expected return for a given level of risk (Markowitz, 1959).

MPT is a method that investors can use to construct diversified portfolios that maximize returns without unacceptable levels of risk. A key component of MPT theory is diversification. Markowitz argued that investors would achieve the best results by evaluating their tolerance for risk and choosing the optimal combination of the two.

Let vector $W = \{w_1, w_2, \cdots, w_n\}$ with n-assets) be the strategy for an investment portfolio consisting of financial assets, where $w_i$is the amount of capital invested in the i-th asset. We assume the distribution of future asset returns and optimize W to maximize the expected portfolio's return and minimize its risk. According to Markowitz, the prediction of the probability distribution of asset return $r$rate following assumptions:

$r \sim N(\mu, \Sigma)$ where r is the return vector (r_i is the return on asset i)

μ is the expected average return vector,

Σ is the covariance matrix.

The expected mean returns μ and the return covariance matrix Σ is estimated from past observations and is assumed to be constant in the future. Given a portfolio strategy W, the portfolio future return $r_p(W)$ is determined by a linear combination of individual asset returns.

$$
\begin{aligned}
r_p(W) &\sim N\left(\mu_p(W), \sigma_p^2(W)\right) \\
\mu_p(W) &= \sum_i w_i \mu_i \\
\sigma_p^2(W) &= \sum_i \sum_j \Sigma_{i,j} w_i w_j
\end{aligned}
\tag{1}
$$

where $\sum_i w_i = 1$.

We aim to find W that minimizes the portfolio risk factor σ and maximizes the expected value μ_p. This optimization problem can be solved in closed form. Generally, the efficient frontier is represented by a solid line in the risk-return space in Figure 1. We use the covariance matrix Σ to reach the efficient frontier and minimize the risk. That is, assets with a small correlation coefficient with other assets should be included. The Markowitz Framework is a mathematically robust model. However, the home has some drawbacks. First, returns on individual assets are not normally distributed. Second, interactions between different assets can be non-linear, but the covariance Σ only captures linear dependencies. Third, future probability distributions of asset returns may differ from past ones.

Insert <Figure 1> here

In this study, we try to solve this problem by using Quantum GAN, a generative model using quantum computers. QuGAN implicitly reflects non-linear interactions between different assets without assuming a probability distribution for the rate of return of development assets. QuGAN also explicitly models the trained current market conditions and future probability distributions of returns.

3. Literature Review

3.1 Portfolio Optimization

MPT is an investment theory that seeks to maximize the expected return of a portfolio for a given amount of portfolio risk or minimize the risk for a given level of expected return by selecting a ratio of different assets. Although MPT is widely used in practice in the financial industry, in recent years, the underlying assumptions of MPT have been extensively challenged.

MPT is an important advance in the mathematical modeling of finance. MPT, also known as portfolio management theory, is a sophisticated investment decision approach that helps investors classify, estimate, and control the type and amount of expected risk and return. Portfolio theory departs from traditional security analysis in that it shifts the emphasis from analyzing the characteristics of individual investments to determining the statistical relationship between the individual securities that make up the overall portfolio (Elton & Gruber, 1997). The theory at the heart of portfolios quantifies the relationship between risk and return and posits that investors should be rewarded for taking the risk. This theory encourages asset diversification to hedge against market risk and risks inherent to a particular company.

MPT mathematically formulates investment diversification, selecting a collection of investment assets that collectively have lower risk than individual assets. This possibility is intuitive to see, as different types of assets often change in value in opposite directions. However, diversification lowers risk even when asset returns are positive, not negatively correlated. More technically, the MPT model's asset returns as a conventionally distributed function (or, more generally, an elliptic distributed random variable), defines risk as the standard deviation of returns, and models a portfolio as a weighted combination of assets. A portfolio is a weighted combination of returns on assets. MPT seeks to reduce the total variance of portfolio returns by combining multiple assets whose returns are not positively correlated. MPT also assumes investors are rational and markets are efficient.

The idea behind MPT is that assets in an investment portfolio should not be individually selected on merit. Instead, it's important to consider how each asset's price changes and all other assets in the portfolio change. An investment is a balance between risk and expected return. For a given risk, MPT describes selecting the portfolio with the highest expected return. Or, for a given expected return rate, MPT describes setting a portfolio with the lowest potential risk. Generally, assets with higher expected returns are riskier (Taleb, 2007).

To overcome the limitations of MPT, a conditional volatility model that can change the volatility of returns over time has been studied. These sophisticated statistical models assume that changing relationships between assets will eventually return to normal. Therefore, long-term changes in returns or correlations fail.

With machine learning advances, investors and researchers are researching to apply machine learning to finance. However, most research focuses on trading strategies using reinforcement learning. These trading strategies focus on decision-making and allow portfolio diversification. Reinforcement learning buys additional assets with increased target weights and sells assets with decreased target

weights. Reinforcement learning assumes an ideal market where all trades are instant and does not affect the market. However, there are thousands of traders trading simultaneously in the market, and complex factors affect the market, given the complexities of financial markets, machine learning, and portfolio management.

The QuGAN algorithm assumes a single agent and an ideal trading environment in this work. Each trade is executed instantly and does not affect the market. Indeed, the trading environment is essentially a multiplayer game with thousands of agents acting simultaneously and influencing the market in complex ways. Combining machine learning with portfolio management still needs to be explored, given the complexities of financial markets.

3.2 QuGAN

Machine learning is being used across society today, from image and voice recognition to traffic prediction, product recommendation, medical diagnosis, stock market trading, and fraud detection. Deep neural networks, a specific machine learning tool, have made significant progress over the past few years. However, despite this progress, such machine learning needs more data sizes. An experiment in the laboratory can be run many times, whereas a time series of stock prices only occurs once in finance. To compensate for this, attention was paid to reproducing existing data with high accuracy.

One of them is a generative adversarial network (GAN). It is an unsupervised learning device in which two neural networks, a generator, and a discriminator, compete to generate information similar to a given data set in the minimax game (Goodfellow et al., 2014). They have been utilized over the past few years in the fields of image generation (Schawinski et al., 2017; Yu et al., 2018), medicine (Anand & Huang, 2018; Zhavoronkov et al., 2019), and quantitative finance (Ruf & Wang, 2020).

A preliminary study exploits the exponential advantages of quantum computing, demonstrating the quality of this approach, especially for high-dimensional data (Huang et al., 2021). Ling et al. (2019) presented experimental proof-of-principle demonstrations of QuGAN in superconducting quantum circuits, Stein et al. (2021) use quantum fidelity measures to propose loss functions acting on quantum states.

Real quantum computers are not yet available, but the Noisy Intermediate-Scale Quantum (NISQ) algorithm already exists and can perform quantum-like tasks (Bharti et al. 2021). Indeed, recently Quantitative Finance has placed a great emphasis on data-driven models (using deep learning and reinforcement learning), and the need for large amounts of data for training purposes has increased. Thus, generative models (Kondratyev and Schwarz 2019) are key in helping generate realistic data that can be used for training.

4. Portfolio optimization with QuGAN

4.1 Overview QuGAN

GAN allows the processing potentially complex financial services data so that the distribution does not need to be explicitly specified. GAN will implicitly maximize the likelihood of complex distributions, allowing us to generate samples from such distributions. The key here is an implicit maximum likelihood estimation principle that does not specify which complex distributions are parameterized.

This study deals with time series data on stock prices. Bai et al. (2018) show that one-dimensional convolutional networks are effective for processing time series and outperforming conventional recurrent networks regarding result quality and performance. In our study, we process the time series and represent it as a matrix M with the number of assets k columns and m rows (dates), $M \in R^{m \times k}$.

So M consists of two parts. M_b is the known part with length b and the past stock price. M_f is the unknown part with length f and the future stock price. A generative deep neural network G is applied to learn the probability distribution of a target future price M_f given a prior distribution of known recent past M_b. Figure 2 shows t graphical interpretation of the inputs and outputs of generator G. A generative model returns a synthesizable future matrix M_f by simulation.

$$M_f = \mathrm{G}(M_b) \tag{2}$$

The known past M_b is used to adjust the probability distribution of the future M_f based on the most updated market conditions. Generator G is a generative network in which M_f learns its weights such that the past M_b matches the probability distribution of given M_f in the training data set. Generator G is trained in adversarial mode against discriminator D to minimize the entropy between synthetic data M_f and real data M_b based on historical observations.

Insert <Figure 2> here

To implement the adversarial training process, we consider a discriminant network D that connects the full price matrix M, namely the condition M_b, and the synthetic data M_f or the real data M_f. The discriminator output is the threshold $c = D(M)$. The discriminator is trained to minimize c for real data and maximize c for synthetic data, whereas Generator G's training goal is to minimize c for synthetic data.

QuGAN is a quantum algorithm used for generative modeling. The algorithm uses the interaction of quantum generators. That is, learn the underlying probability distribution given ansatz

and classical discriminators, neural networks, and training data.

QuGAN distinguishes between real and generated distributions. Like GAN, generators and discriminators of QuGAN are trained in alternating optimization steps. The generator aims to generate samples that the discriminator will classify as training data samples, and the discriminator is the initial training to try to differentiate. The end goal is for the quantum generator to learn a representation of the underlying probability distribution of the training data. Thus, a trained quantum generator can load quantum states that are approximate models of the target distribution.

4.2 QuGAN architecture

Normalize the return at closing price p, adjusted over the training period. We use a revised closing price p for each financial asset. Generally, $[0,1]$ is used primarily for regularization in machine learning. However, in this study, it is normalized to $[-1,1]$ to distinguish the rise and fall of the stock price easily. This normalization allows limited values to be learned to a reasonable level. However, in this case, data for outliers is also normalized, so in actual learning, data for the top 5% and bottom 5% are excluded and normalized.

$$normalized\ r\ = \left(\frac{2}{r_{max} - r_{min}}\right)(r - r_{min}) - 1 \tag{3}$$

where, r_{max} and r_{min} mean the maximum and minimum values of the rate of return for a given asset, respectively.

Given stock data, we use QuGAN to learn the underlying random distribution of the data and directly load it into a quantum state.

$$|g_{trained}\rangle = \sum_{j=1}^{2^n-1} \sqrt{p_j}|r_j\rangle \tag{4}$$

where $\sqrt{p_j}$ is the probability amplitude of the $|r_j\rangle$. In other words, the probability of getting state $|r_j\rangle$ is a p_j. The main goal of QuGAN is to generate a probability distribution close to the underlying distribution of training data M (Zoufal et al., 2019).

As with other quantum algorithms, samples must be mapped to discrete values. The number of values that can be expressed is determined by the number of qubits used. Therefore, the density of data is defined as the number of qubits. The n-qubits can represent 2^n discrete data.

When the learning process is complete, the generator G can synthesize a realistic future price $M_f\ =\ G(M_b)$. We use these synthetic simulations to numerically estimate the expected risk and return

for different portfolio diversification strategy w. Therefore, we run portfolio optimization on the estimated posterior probability distribution.

For a given conditioning M_b, let us consider a set S of n simulations $M_f \in$ S sampled at $P(M_f \mid M_b)$ by evaluating the generative model $G(M_b)$. Portfolio return achieved with diversification w for a given the simulation M_f is:

$$r_p(w, M_f) = \sum_i x_i \, r_i(M_f) \tag{5}$$

A simulation $M_f \in S$ sampled from the probability distribution $P(M_f \mid M_b)$ is used to infer the probability. The portfolio optimization problem is defined as in the traditional Markowitz's optimization approach (Section II), but runs on the predicted future probability distribution, which is nonnormal and contains nonlinearities. Interactions between different assets. For example, the optimization goal is to identify the configuration of x that maximizes the expected return $\mu_p = E(r_p(w, M_f) \mid w, M_b)$ and minimizes the risk function $\sigma(w, M_b)$. Both σ and μ_p are estimated based on simulated samples $M_f \in S$.

In this framework, the risk function $\sigma(\cdot)$ can be any metric such as risk value or volatility. Without loss of generality, we use estimated volatility, which allows the approach to be directly evaluated with respect to traditional Markowitz's methodology. So, the optimization problem follows as below:

$$\begin{aligned} &\max_w \mu_p(w|S) \\ &\min_w \sigma(w|S) \end{aligned} \tag{6}$$

Equation (5) is the objective function. We solve optimization problem like MPT.

Figure 3 shows the quantum circuit for QuGAN. The number of dimensions and the number of distributions to discretize determine the number of qubits. For example, if the number of assets is three and each asset has four qubits (discrete with a total distribution of 2^4), we need 12 qubits.

Insert <Figure 3> here

5. Numerical Result

5.1 Data select

To evaluate the proposed QuGAN approach, we apply publicly available data, from Yahoo Finance.[1] Our test uses three-year data from January 2019 to December 2021, stock price data. A generative model G is trained using the daily returns of individual stocks. This learned model is used to optimize the portfolio. The summary statistics of the daily stock return are reported in Table 1. The number of observations is 756.

Insert <Table 1> here

In this task, we construct a portfolio using three individual stocks, Apple, Google and Amazon. We select three stocks taking into account the following considerations. First, we include only assets for which data is available from at least 2010, according to the Yahoo Finance data source. Yahoo Finance found some erroneous data, such as NaN values or 10-fold fluctuations in asset prices in one day, etc. These errors are rare, but related assets were excluded.

Insert <Figure 4> here

The portfolio under consideration comprises stocks with low correlations and asset price volatility. Figure 4 shows the time series of the stock price and daily return from January 2019 to December 2021. When building a portfolio, it should be made up of assets with low correlations. This is because it can reduce volatility while maintaining maximum returns. Figure 5 shows the correlation matrix with real market data. The heat map below is the correlation coefficient for three stocks: Apple, Google, and Amazon. The closer the correlation coefficient is to one, the more assets move together. The correlation coefficient between Apple and Google is the highest at 0.12; the correlation is close to zero.

Insert <Figure 5> here

5.2 Benchmarks

We benchmark the proposed QuGAN approach with respect to Markowitz's state-of-the-art portfolio optimization (Rubinstein, 2002). QuGAN algorithm returns a discrete set of optimal diversifications $w \in X$, whereas Markowitz's methodology solves the optimization problem in continuous form. In this work, we define a random portfolio of 10,000. Therefore, the return and risk of the i-th portfolio is defined by Equation (1).

[1] https://finance.yahoo.com/

Figure 6 shows the measured and ranked Sharpe Ratio with real market data. The higher the weight for Apple, the higher the Sharpe Ratio, the higher the weight for Amazon, the lower the Sharpe Ratio. Figure 7 is the scatter plot of each portfolio by returning the portfolio's risk on the x-axis and the y-axis.

Insert <Figure 6> here

Insert <Figure 7> here

5.3 Portfolio analysis with QuGAN

QuGAN learns from real data and creates fake market data. Figures 8 and 9 show the results of comparing the distribution of fake data generated in this way with real data. Figure 8 is the distribution using actual data. All three assets it has the same shape as the normal distribution. Figure 9 is a histogram of fake data generated through QuGAN. Since the actual discretization is divided into 16 intervals, a curve is seen compared to the original distribution.

Insert <Figure 8> here

Insert <Figure 9> here

The methodological limitations of GANs and incomplete quantum computers cause this error (Preskill, 2018; Wang et al., 2017). This issue makes the correlation coefficient of fake data higher. Figure 10 shows the correlation under fake data. This correlation is higher than the correlation in Figure 5.

Insert <Figure 10> here

We apply the same methodology in Section 4.2 using this fake data. Based on the weights applied to the portfolio in Section 4.2, returns and risks are measured and ranked by applying them to fake data. Figure 11 shows the rank of 10,000 random portfolios by measuring the Sharp Ratio. Using real market data, a higher weighting of Apple would result in a higher Sharp Ratio, and a higher weighting of Amazon would result in a lower Sharp Ratio. This contrasts the higher Sharp Ratio when Google's proportion is higher when using actual market data.

Insert <Figure 11> here

We show the return and risk of the portfolio created in this way on a scatter plot in Figure 12.

This figure shows that an efficient frontier using real data has a higher return with less risk.

Insert <Figure 12> here

6. Conclusion

We train a GuGAN model and compare it to Markowitz. This reference approach is deterministic and will always produce the same result given the training data. Proceed as follows. Given a trained QuGAN model, we analyze the return risk of QuGAN diversification during a test period and compare the results with the diversification proposed by Markowitz. Markowitz and QuGAN diversification at risk are associated returns. QuGAN can overcome Markowitz's difficulty in modeling long-term situations.
QuGAN has two drawbacks. GANs are known to be unstable, and adversarial training often does not converge toward equilibrium due to the nonlinear dynamics introduced by the differential equations that implement the learning algorithm. Quantum computers also do not exist as perfect machines and assume quantum errors.

Nonetheless, this work presents a pioneering study on portfolio analysis using QuGAN. We use quantum computers as a diversification strategy to optimize portfolios to minimize risk and maximize expected returns. The key novelty is that the proposed approach addresses a growing problem in the high-efficiency market. That is, there is no need to predict medium- to long-term price trends, assuming that all currently available information is already indicated in current asset prices.

Results show clear advantages in the Cutting Edge of Portfolio Optimization Theory. In particular, the proposed approach can expose end-users to the possibility of choosing a target risk level and suggest specific diversification in current market conditions.

This study has limited access to actual quantum computers. In future research, it is expected that using real quantum computers will improve the learning and accuracy of vast data.

Reference

Anand, N., & Huang, P. (2018). Generative modeling for protein structures. *Advances in Neural Information Processing Systems*, *31*. Curran Associates, Inc.

Assouel, A., Jacquier, A., & Kondratyev, A. (2022). A quantum generative adversarial network for distributions. *Quantum Machine Intelligence*, *4*, 28.

Bai, S., Kolter, J. Z., & Koltun, V. (2018, April 19). *An Empirical Evaluation of Generic Convolutional and Recurrent Networks for Sequence Modeling*. arXiv.

Elton, E. J., & Gruber, M. J. (1997). Modern portfolio theory, 1950 to date. *Journal of Banking & Finance*, *21*, 1743–1759.

Goodfellow, I. J., Pouget-Abadie, J., Mirza, M., Xu, B., Warde-Farley, D., Ozair, S., … Bengio, Y. (2014, June 10). *Generative Adversarial Networks*. arXiv.

Huang, H.-L., Du, Y., Gong, M., Zhao, Y., Wu, Y., Wang, C., … Pan, J.-W. (2021). Experimental Quantum Generative Adversarial Networks for Image Generation. *Physical Review Applied*, *16*, 024051.

Jaeger, M., Krügel, S., Marinelli, D., Papenbrock, J., & Schwendner, P. (2020, January 30). *Understanding Machine Learning for Diversified Portfolio Construction by Explainable AI* [SSRN Scholarly Paper]. Rochester, NY. https://doi.org/10.2139/ssrn.3528616

Krizhevsky, A., Sutskever, I., & Hinton, G. E. (2017). ImageNet classification with deep convolutional neural networks. *Communications of the ACM*, *60*, 84–90.

Ling, H., Wu, S., Cai, W., Ma, Y., Mu, X., Xu, Y., … Sun, L. (2019). *Quantum generative adversarial learning in a superconducting quantum circuit*. *2019*, E27.005.

Markowitz, H. M. (1959). *Portfolio Selection: Efficient Diversification of Investments*. Yale University Press.

Preskill, J. (2018). Quantum Computing in the NISQ era and beyond. *Quantum*, *2*, 79.

Rubinstein, M. (2002). Markowitz's "Portfolio Selection": A Fifty-Year Retrospective. *The Journal of Finance*, *57*, 1041–1045.

Ruf, J., & Wang, W. (2020, May 9). *Neural networks for option pricing and hedging: A literature review*. arXiv.

Schawinski, K., Zhang, C., Zhang, H., Fowler, L., & Santhanam, G. K. (2017). Generative adversarial networks recover features in astrophysical images of galaxies beyond the deconvolution limit. *Monthly Notices of the Royal Astronomical Society. Letters*, *467*, L110–L114.

Stein, S. A., Baheri, B., Chen, D., Mao, Y., Guan, Q., Li, A., … Xu, S. (2021). QuGAN: A Quantum State Fidelity based Generative Adversarial Network. *2021 IEEE International Conference on Quantum Computing and Engineering (QCE)*, 71–81.

Taleb, N. N. (2007). *The Impact of the Highly Improbable*.

Timmermann, A., & Granger, C. W. J. (2004). Efficient market hypothesis and forecasting. *International Journal of Forecasting*, *20*, 15–27.

Tsay, R. S. (2005). *Analysis of Financial Time Series*. John Wiley & Sons.

Wang, K., Gou, C., Duan, Y., Lin, Y., Zheng, X., & Wang, F.-Y. (2017). Generative adversarial networks: Introduction and outlook. *IEEE/CAA Journal of Automatica Sinica*, *4*, 588–598.

Yu, J., Lin, Z., Yang, J., Shen, X., Lu, X., & Huang, T. S. (2018, June 1). *Generative Image Inpainting with Contextual Attention*. 5505–5514. IEEE Computer Society.

Zhavoronkov, A., Ivanenkov, Y. A., Aliper, A., Veselov, M. S., Aladinskiy, V. A., Aladinskaya, A. V., … Aspuru-Guzik, A. (2019). Deep learning enables rapid identification of potent DDR1 kinase inhibitors. *Nature Biotechnology*, *37*, 1038–1040.

Zoufal, C., Lucchi, A., & Woerner, S. (2019). Quantum Generative Adversarial Networks for learning and loading random distributions. *Npj Quantum Information*, *5*, 1–9.

<Appendix> Table & Figure

Table 1. Summary of statistics

This table reports the daily stock return summary statistics from January 2019 to December 2021. The number of observations is 755.

index	Apple	Google	Amazon
count	755	755	755
mean	0.002269	0.001526	0.001211
std	0.021506	0.018668	0.018513
min	-0.128647	-0.116341	-0.079221
25%	-0.00751	-0.006339	-0.00841
50%	0.001786	0.001694	0.00134
75%	0.013234	0.010331	0.010611
max	0.119808	0.096202	0.079295

Figure 1. Efficient frontier with risky assets

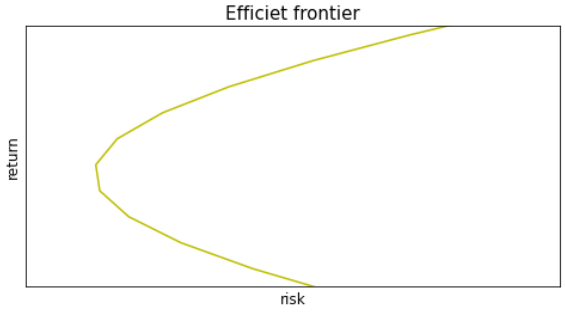

Figure 2. Diagram of QuGAN algorithm

This figure is a schematic diagram of a series of processes for QuGAN.

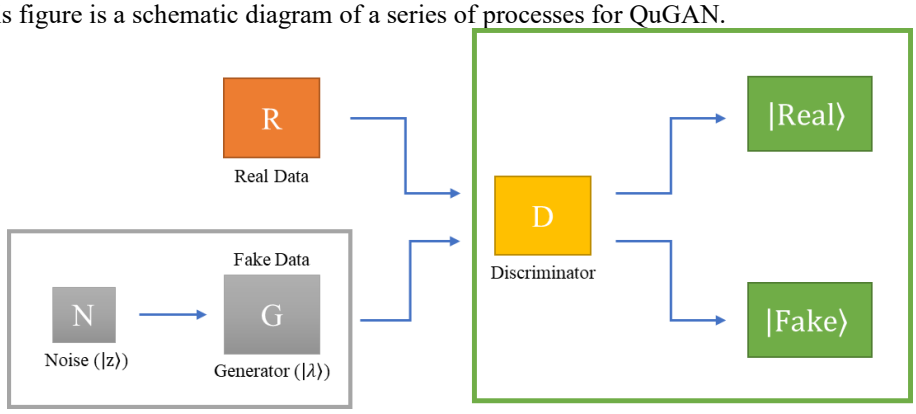

Figure 3. Quantum circuit of QuGAN

This figure is a schematic diagram of a series of processes for QuGAN.

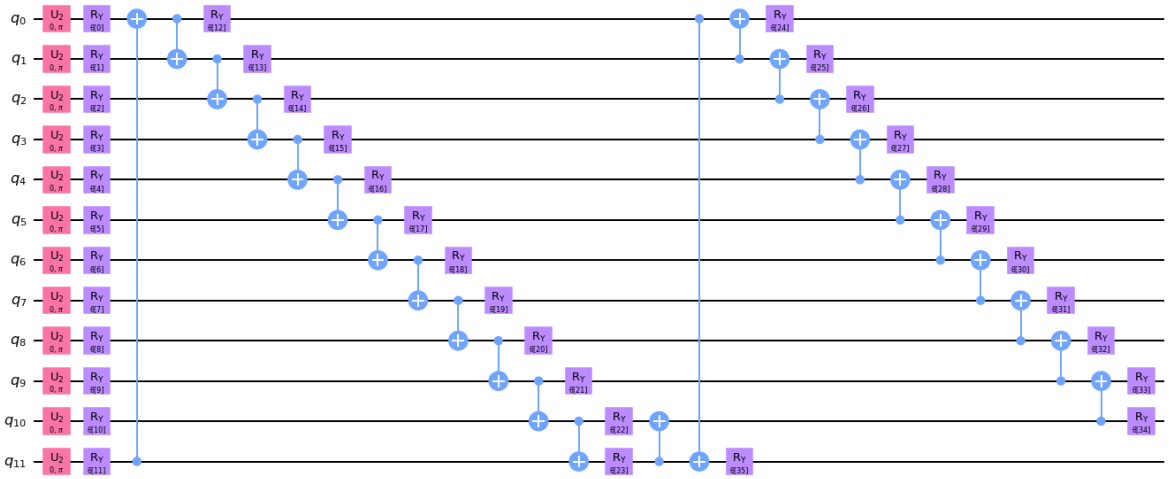

Figure 4. Time Series of stock price and daily return

This figure shows the time series of the stock price and daily return from January 2019 to December 2021.

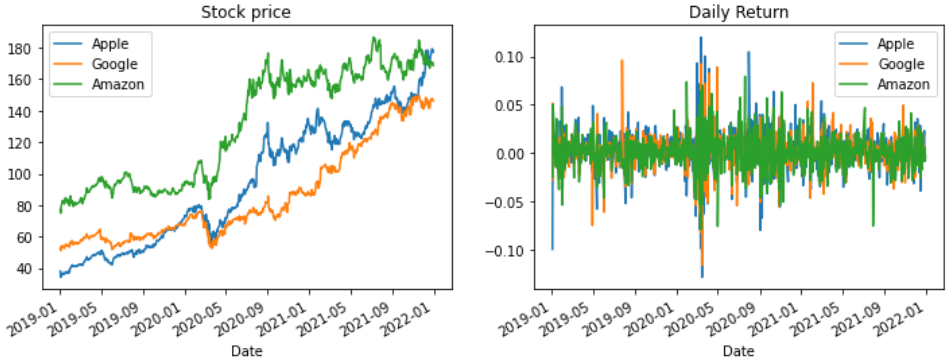

Figure 5. Correlation between 3 stocks

This figure shows the correlation matrix with real market data from January 2019 to December 2021. When building a portfolio, it should be made up of assets with low correlations. This is because it can reduce volatility while maintaining maximum returns. The heat map below is the correlation coefficient for three stocks: Apple, Google, and Amazon. The closer the correlation coefficient is to 1, the more assets move together. The correlation coefficient between Apple and Google is the highest at 0.12; the correlation is close to 0.

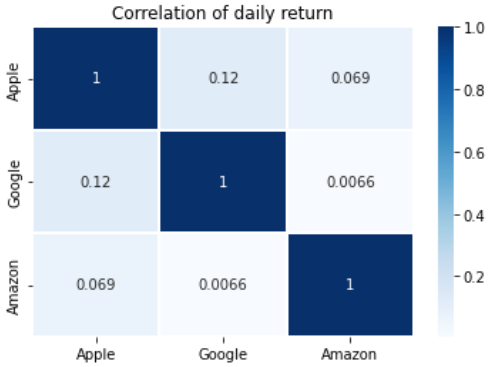

Figure 6. Ranking of optimal portfolios by Sharp Ratio

This figure shows the ranking of 10000 random portfolios by measuring the Sharp Ratio. In the case of using actual market data, the higher the proportion of Apple, the higher the Sharp Ratio, and the higher the proportion of Amazon, the lower the Sharp Ratio.

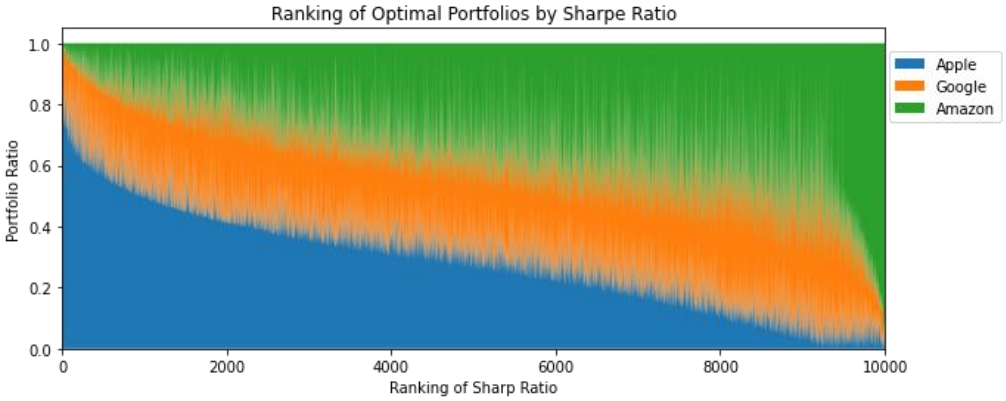

Figure 7. Optimal portfolio with real market data

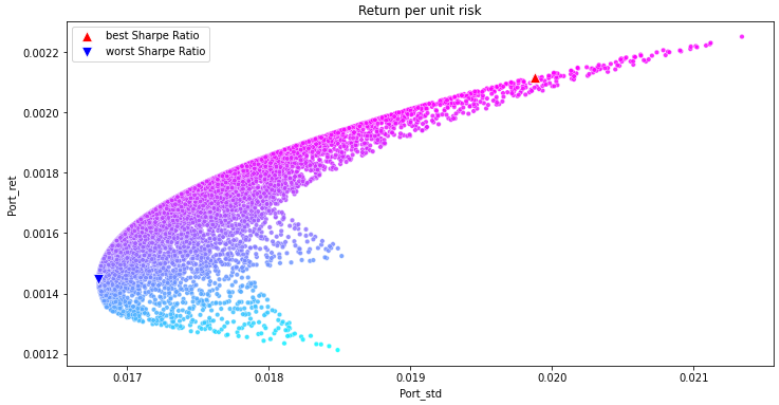

Figure 8. Histogram of daily return with real market data

This figure shows the histogram of daily returns from January 2019 to December 2021. All histograms have the shape of a normal distribution.

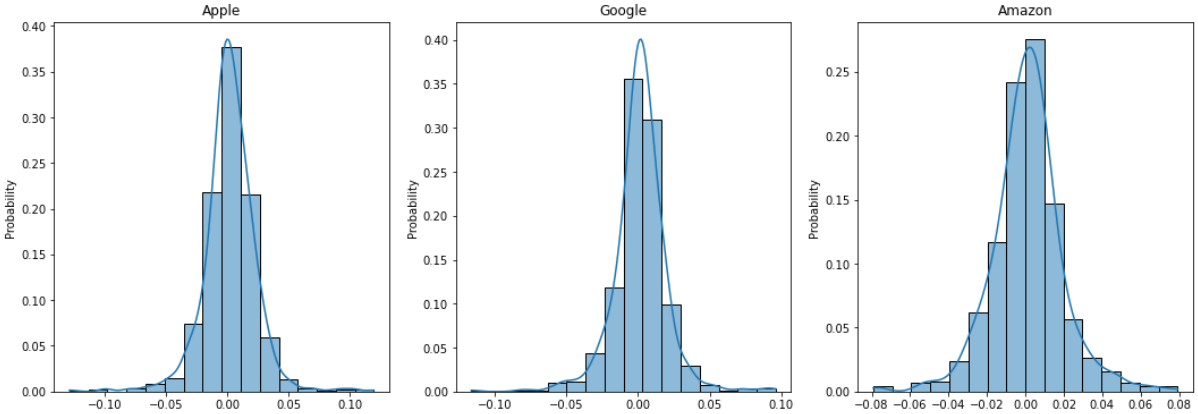

Figure 9. Histogram of daily return with QuGAN

This figure shows the histogram of daily returns with QuGAN. The sample is 1510 data.

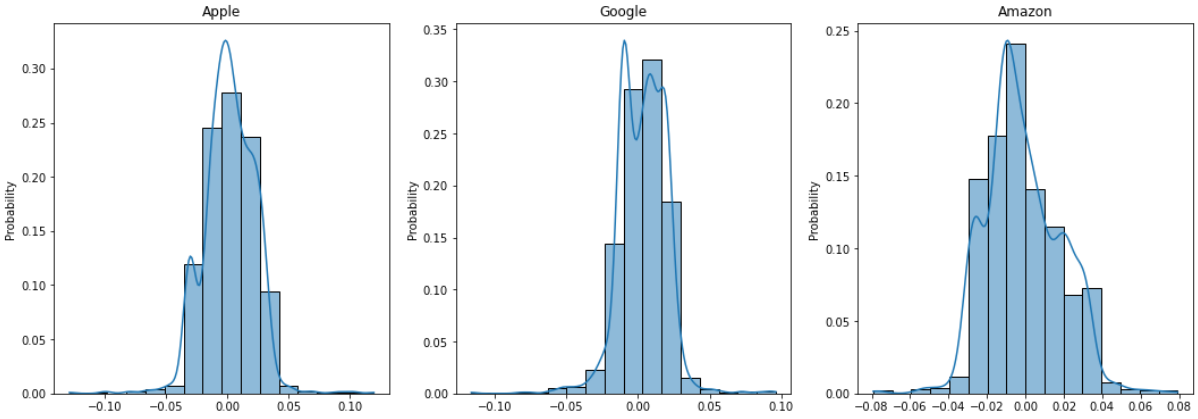

Figure 10. correlation of three assets with QuGAN

This figure shows a correlation matrix with fake market data. The heatmap below shows the correlation coefficients for Apple, Google, and Amazon stocks. QuGAN's correlation is higher than that of real market data.

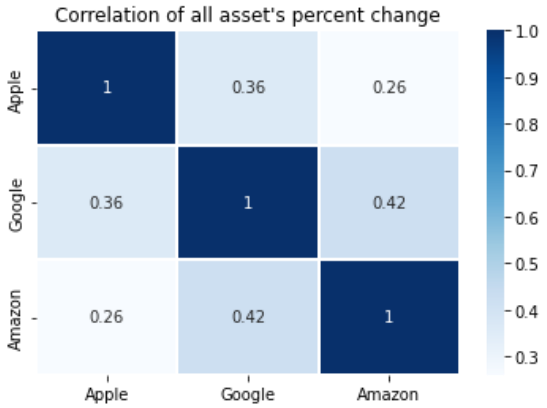

Figure 11. Ranking of Optimal Portfolio by Sharp Ration with QuGAN

This figure shows the ranking of 10000 random portfolios by measuring the Sharp Ratio. In the case of using actual market data, the higher the proportion of Apple, the higher the Sharp Ratio, and the higher the proportion of Amazon, the lower the Sharp Ratio.

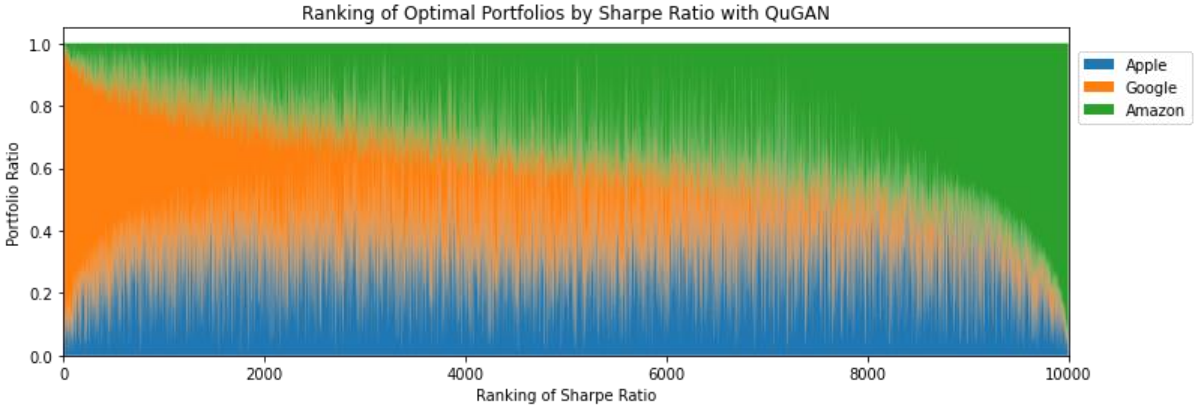

Figure 12. Return per unit risk with QuGAN